NIH Public Access
Author Manuscript
J Med Chem. Author manuscript; available in PMC 2014 March 27.

Published in final edited form as:
J Med Chem. 2012 November 26; 55(22): 9973–9987. doi:10.1021/jm301212u.

Lead Discovery, Chemistry Optimization, and Biological Evaluation Studies of Novel Biamide Derivatives as CB_2 Receptor Inverse Agonists and Osteoclast Inhibitors

Peng Yang[†,§,×], **Kyaw-Zeyar Myint**[†,‡,§,×], **Qin Tong**[†,§], **Rentian Feng**[†,§], **Haiping Cao**[†], **Abdulrahman A. Almehizia**[†,§], **Mohammed Hamed Alqarni**[†,§], **Lirong Wang**[†,§,‖], **Patrick Bartlow**[†,§], **Yingdai Gao**[#], **Jürg Gertsch**[∞], **Jumpei Teramachi**[•], **Noriyoshi Kurihara**[•], **Garson David Roodman**[•], **Tao Cheng**[#], and **Xiang-Qun Xie**[*,†,‡,§,‖,⊥]

[†]Department of Pharmaceutical Sciences and Computational Chemical Genomics Screening Center, School of Pharmacy, University of Pittsburgh, Pittsburgh, Pennsylvania 15260, United States [‡]Department of Computational and Systems Biology, University of Pittsburgh, Pittsburgh, Pennsylvania 15260, United States [§]Drug Discovery Institute, University of Pittsburgh, Pittsburgh, Pennsylvania 15260, United States [‖]Pittsburgh Chemical Methods and Library Development Center, University of Pittsburgh, Pittsburgh, Pennsylvania 15260, United States [⊥]Department of Structural Biology, University of Pittsburgh, Pittsburgh, Pennsylvania 15260, United States [#]State Key Laboratory of Experimental Hematology, Institute of Hematology and Blood Diseases Hospital, Chinese Academy of Medical Sciences and Peking Union Medical College, Tianjin 300020, P. R. China [∞]Institute of Biochemistry and Molecular Medicine, University of Bern, Bühlstrasse 28, CH-3012 Bern, Switzerland [•]School of Medicine, Indiana University, Indianapolis 46202, Indiana

Abstract

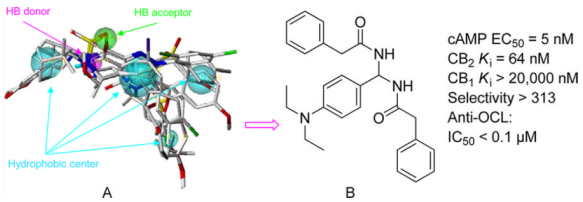

N,*N*′-((4-(Dimethylamino)phenyl)methylene)bis(2-phenylacetamide) was discovered by using 3D pharmacophore database searches and was biologically confirmed as a new class of CB_2 inverse agonists. Subsequently, 52 derivatives were designed and synthesized through lead chemistry optimization by modifying the rings A–C and the core structure in further SAR studies. Five compounds were developed and also confirmed as CB_2 inverse agonists with the highest CB_2 binding affinity (CB_2 K_i of 22–85 nM, EC_{50} of 4–28 nM) and best selectivity (CB_1/CB_2 of 235- to 909-fold). Furthermore, osteoclastogenesis bioassay indicated that PAM compounds showed great inhibition of osteoclast formation. Especially, compound **26** showed 72% inhibition activity even at the low concentration of 0.1 μM. The cytotoxicity assay suggested that the inhibition of PAM compounds on osteoclastogenesis did not result from its cytotoxicity. Therefore, these PAM

© 2012 American Chemical Society

[*]**Corresponding Author** Phone: +1-412-383-5276. Fax: +1-412-383-7436. xix15@pitt.edu.
[×]These authors made equal contributions to this work.

The authors declare no competing financial interest.

NIH-PA Author Manuscript
NIH-PA Author Manuscript
NIH-PA Author Manuscript

NIH-PA Author Manuscript

NIH-PA Author Manuscript

NIH-PA Author Manuscript

derivatives could be used as potential leads for the development of a new type of antiosteoporosis agent.

INTRODUCTION

In the past decades, cannabinoid research has witnessed significant evolution, including the discoveries of cannabinoid (CB) receptors, their endogenous ligands, the putative anandamide membrane transporter (AMTa)[1] for endocannabinoid cellular uptake and inactivation, the fatty acid amide hydrolase (FAAH),[2] and the monoacylglycerol lipase (MAGL)[3] enzymes responsible for CB ligand metabolisms. Among the discovered cannabinoid receptors, the subtypes CB_1 and CB_2 share 48% identity at the amino acid level[4,5] and belong to the rhodopsin-like family class A of G-protein-coupled receptors (GPCRs). While the location of the CB receptor subtypes is recently being debated,[6–8] it is believed that the CB_1 receptor is expressed predominantly in the brain (central receptor for cannabinoids)[4] and the CB_2 receptor in peripheral cells and tissues derived from the immune system (peripheral receptor for cannabinoids).[5]

Importantly, the discovered endocannabinoid system is known to play a key role in numerous biological processes and exhibits pharmacological effects in a large spectrum of diseases and disorders, such as pain,[9] immune and inflammatory disorders,[10,11] cancer,[12,13] osteoporosis,[14] and cardiovascular and gastrointestinal disorders.[15–17] While the investigations were aimed at designing new synthetic molecules that target cannabinoid receptors in past years, cannabinoid (CB) drug research is experiencing a challenge, as the CB_1 antagonist rimonabant, launched in 2006 as an anorectic/antiobesity drug, was withdrawn from the European market because of complications of suicide and depression side effects. These undesirable central nervous system side effects are thought to be CB_1-receptor-mediated.[18] Thus, strategic medicinal chemistry design is needed to develop CB_2 selective ligands for therapeutic medications without undesirable side effects.

The therapeutic potential of CB_2 receptor modulation has prompted the development of CB_2 receptor selective ligands, either as agonists or as antagonists/inverse agonists. Several reviews,[19–23] including the latest review from our lab,[23] summarize the advances of new CB_2 ligands from literature and patents (Figure 1). The first CB_2 inverse agonist discovered is **1** (SR144528).[24] This compound and **2** (AM630)[25] have been extensively used as standards to measure the specificity of various cannabinoid agonists for CB_2 in animal models. **3** (JTE-907)[26] and **4** (Sch225336)[27] received much attention for their immunomodulatory properties against inflammatory disorders in which leukocyte recruitment is involved. Recently, the natural product **5** (MH)[28] and several derivatives were shown to selectively target CB_2 receptors and act as inverse agonists with anti-inflammatory and antiosteoclastogenic properties. In addition, the pyrimidine derivative **6** (GW842166X) was found to be a potentially promising therapeutic agent for the treatment of inflammatory and neuropathic pain.[29] More recently, it was reported that **7** (JWH-133) dose-dependently inhibited intravenous cocaine self-administration, cocaine-enhanced locomotion, and cocaine-enhanced accumbens extracellular dopamine in wild-type and CB_1 receptor knockout mice.[30] This result suggests that brain CB_2 receptors may be a drug target for the pharmacotherapy of drug abuse and addiction. Moreover, the natural product **8** ((E)-β-caryophyllene [(*E*)-BCP]) was identified as a functional nonpsychoactive CB_2 receptor ligand and as a macrocyclic anti-inflammatory cannabinoid in *Cannabis*.[31] Taken together, these published studies show that the CB_2 receptor is an attractive target for developing potentially therapeutic ligands.

NIH-PA Author Manuscript

NIH-PA Author Manuscript

NIH-PA Author Manuscript

In order to discover novel CB_2 selective inverse agonists, we used the genetic algorithm-based pharmacophore alignment (GALAHAD, SYBYL 8.0) approach to derive active pharmacophore models based on the reported CB_2 inverse agonists, including **1–4** (Figure 1). A representative pharmacophore model was illustrated in Figure 2, showing one H-bond (HB) acceptor (green), one HB donor (pink), and four hydrophobic (light blue) features. We then performed a 3D database search using the defined pharmacophore query via the UNITY pharmacophore search program (SYBYL 8.0), and identified compound **9** (*N*,*N*′-((4-(dimethylamino)phenyl)methylene)-bis(2-phenylacetamide)) (Xie95 or PAM, Figure 2B) as a novel chemotype with selective CB_2 activity (CB_2 K_i = 777 nM, selectivity index of >26-fold) validated by [^{3}H]CP-55040 radiometric binding assays. On the basis of this promising result, we chose compound **9** as a prototype for further SAR medicinal chemistry studies. In this report, we have designed and synthesized a series of novel PAM derivatives (Scheme 1). Binding activities and effects of these derivatives on the CB_2 receptor downstream cAMP production have also been investigated to define their structure–activity relationships and ligand functionality. Our systematic studies led to the identification of five new derivatives (Figure 3) as novel CB_2 selective ligands with improved CB_2 binding affinity and high selectivity. Importantly, some showed promising inhibition activity to osteoclast cells derived from human bone marrow. The toxicity of PAM compounds on normal human mononuclear cells was also investigated.

RESULTS AND DISCUSSION

Pharmacophore Modeling and Virtual Screening

A representative 3D pharmacophore model was derived via a genetic algorithm-based pharmacophore alignment method (GALAHAD)[32,33] using a set of known CB_2 inverse agonists/antagonists including **1, 2, 3**, and **4** (Figure 1). The model was then refined and analyzed using our in-house training database that contained non-CB_2 ligands and active CB_2 ligands. As shown in Figure 2, the final model consisted of one H-bond (HB) acceptor (green), one HB donor (pink), and four hydrophobic (light blue) features. Subsequently, the model was used as a pharmacophore query to screen our in-house structurally diverse chemical database of 540 000 compounds that was constructed from a parent database containing 5.3 million compounds constructed using our published cell-based partition chemistry-space matrix calculation algorithm.[34] Out of top ranked 40 compounds, 20 of them were available commercially or via material transfer agreement and then experimentally tested for CB_2 binding affinity and selectivity. Among experimentally validated compounds, there were three compounds with good CB_2 binding affinities including our lead compound **9**.

Pharmacology and SAR Analysis

On the basis of the lead discovered, we have carried out medicinal chemistry modification and synthesized 52 analogues. The binding affinities of these 52 derivatives to CB_2 were determined by performing [^{3}H] CP-55,940 radioligand competition binding assays using membrane protein preparations of CHO cells stably expressing human CB_2 receptor. The CB_1 binding assay was also conducted for those compounds with high CB_2 receptor binding potency (K_i < 1000 nM) using membrane proteins harvested from the CHO cells stably transfected with the human CB_1 receptor. CB_2 selective ligand **1** (SR144528, CB_2 inverse agonist) and CB_1 ligand **10** (SR141716, CB_1 inverse agonist)[35] were used as positive controls along with the tested compounds in bioassays experiments. The chemical structures, physiochemical properties, binding activities, and selectivity index are summarized in Tables 1–5.

NIH-PA Author Manuscript

NIH-PA Author Manuscript

NIH-PA Author Manuscript

First, the SAR study was focused on the effect of the side chains on aromatic ring C. Twenty-one compounds were synthesized (**11–31**, Table 1). The aromatic ring C was modified with substituents that varied in their size, electronic character, and position. Removal of the *p*-dimethylamino group (compound **11**, CB_2 K_i = 9930 nM) dramatically decreased the CB_2 binding activity. Introducing fluorine atoms to different positions of ring C also lowered the CB_2 receptor affinity (compounds **12–14**, CB_2 K_i of 35 330,12 670, and 10 900 nM, respectively). The CB_2 receptor binding affinities of the F-substituted compounds decreased in the order of *o*-F < *m*-F < *p*-F. From these results, we deduced that substitution at the para position of the phenyl ring may play an important role in the CB_2 receptor binding activity. This deduction was also confirmed by compounds **22** and **23**. Compound **23** bearing *p*-trifluoromethyl showed improved activity (**23**, CB_2 K_i = 596 nM), while compound **22** bearing *o*-trifluoromethyl showed dramatically decreased activity (**22**, CB_2 K_i = 11780 nM). Moreover, replacing the *p*-fluorine with chlorine (compound **15**) or bromine (compound **16**) relatively increased the activity, but the binding affinities were still weak. While introduction of a methyl group to the para position (compound **17**) improved CB_2 receptor affinity, unfortunately, compound **17** also had high affinity for the CB_1 receptor, the only compound that exhibited significant CB_1 receptor binding activity among the 52 compounds (**17**, CB_1 K_i = 109 nM; CB_2 K_i = 494 nM). Replacement of *p*-dimethylamino group with bioisostere isopropyl (compound **18**) dramatically improved the binding activity and selectivity (CB_2 K_i = 85 nM, selectivity index of >235).

As for the compounds with alkoxy groups (compounds **19–21**), the compound bearing methoxy (**19**) showed similar activity and selectivity compared to the parent compounds, the compound bearing ethoxy (**20**) showed slightly decreased activity, and the compound bearing isopropoxy **(21**) showed slightly increased activity. This result indicated that various alkoxy groups were tolerated, but their activity and selectivity for the CB_2 receptor were sensitive to the group size. To explore the electronic and steric effects on CB_2 binding activity, we introduced a nitro group to the benzene ring (**24**), but compound **24** completely lost its binding affinity to CB_2. Reduction of compound **24** to the corresponding amine resulted in compound **25**, which displayed relatively improved activity but was still weak. Replacement of the amine with a diethylamine group, however, resulted in a promising compound (**26**), which showed much improved activity and selectivity compared to the lead compound (CB_2 K_i = 64 nM, selectivity index of >313). When the *p*-diethylamino group was identified as a better chemical group on ring C, additional substituted amino groups were further studied, resulting in several potent compounds **27–31** with *p*-dipropylamino, *p*-dibutylamino, *p*-pyrrolidinyl, *p*-piperidyl, and *p*-dibenzylamino, respectively. Compared with the lead compound **9**, these five compounds showed greatly improved activity and selectivity (CB_2 K_i of 22–595 nM, selectivity index of 34–909). When compared to compound **26** bearing a diethylamino group, compound **27** with a *p*-dipropylamino group showed the most potential binding affinity and selectivity (CB_2 K_i = 22 nM, selectivity index of >909). Compound **30** with a *p*-pyrrolidinyl group showed similar activity (CB_2 K_i = 71 nM, selectivity index of >28l). The modification result showed that CB_2 binding affinity decreased as the size of the functional group at the para position of the benzene ring C increased (compounds **28, 29**, and **31**). Hence, we conclude that the substituted amino group at the para position plays a significant role in CB_2 receptor binding activity and the *p*-dipropylamino group is optimal.

Subsequently, the SAR was further explored on the variation on aromatic rings A and B by introducing Cl or CF_3, resulting in two series of compounds: **32–40** and **41–47**. Among the first series compounds bearing Cl on rings A and B (**32–40**), five compounds (35–39) showed increased CB_2 binding affinity and selectivity. All the compounds with CF_3 on rings A and B in the second series (**41–47**) showed no binding activity to CB_2 receptors. The

NIH-PA Author Manuscript

NIH-PA Author Manuscript

NIH-PA Author Manuscript

results indicated that *p*-Cl is a better substituent than CF_3 and H on rings A and B. Comparison of compound **38** with *o*-CF_3 and compound **39** with *p*-CF_3 further indicates that the para position of the phenyl ring C plays an important role in the CB_2 binding activity.

In addition, the distance from ring C to the methylene amide group as well as from rings A and B to the amide group was also explored (compounds **48–50**, Table 2; compound **51–53**, Table 3). The data indicated that inserting CH_2 (compound **48**), CH_2CH_2 (compound **49**), or CH=CH double bond (compound **50**) between ring C and methylene amide group resulted in a complete loss of activity or weak binding affinity. While removing CH_2 from compound **26** or inserting CH_2CH_2 (compound **52**) or CH=CH double bond (compound **53**) between rings A/B and the methylene amide group led to a slight decrease in binding affinity, these compounds still showed good CB_2 binding affinity and selectivity ($167 \leq CB_2\ K_i \leq 688$ nM; $29 \leq$ selectivity index ≤ 119).

Furthermore, the importance of aromatic ring C in the CB_2 binding activity was explored (compounds **54** and **55**, Table 4). Replacing ring C with alkyl chain butyl (**54**) or pentyl (**55**) led to a complete loss of activity or very weak binding affinity. We conclude that the aromatic ring C plays a significant role in CB_2 receptor binding affinity and may be an essential element to retain activity.

After discovering the importance of the aromatic ring C for CB_2 binding affinity, we then explored the importance of rings A and B by replacing aromatic rings A and B with different alkyl chains (compounds **56–61**, Table 5). The results indicated that replacing the benzyl group with a branched chain isopropyl (compound **56**) or *tert*-butyl group (compound **57**) dramatically decreased the CB_2 binding affinity, whereas replacing the benzyl group with a long alkyl chain butyl (compound **58**) showed slightly decreased affinity. Interestingly, replacement of benzyl with the straight chain pentyl group led to another promising compound **59**, which showed greatly improved binding affinity and selectivity ($CB_2\ K_i = 25$ nM, selectivity index of >800). To further explore the effect of the alkyl chain, we also replaced aromatic rings A and B with longer chains *n*-C_7H_{15} (compound **60**) and *n*-C_9H_{19} (compound **61**). Compared to compound **59**, however, they both showed slightly decreased binding affinity (**60**, $CB_2 K_i = 146$ nM, selectivity index of >136; **61**, $CB_2\ K_i = 160$ nM, selectivity index of > 125). From these results, we conclude that the aromatic rings A and B may be replaced by an alkyl chain and the pentyl group is optimal.

Cell-Based Functional Bioassay in Vitro

Cellular bioassay was carried out using our published protocol[36] to measure the agonistic or antagonistic functional activities of the CB_2 selective compounds. Briefly, the cell-based LANCE cAMP assays were performed on 384-well plates using CHO cells stably expressing the CB_2 receptors in the presence of phosphodiesterase inhibitor RO20-1724 and adenyl cyclase activator forskolin. Since CB_2 is a $G_{\alpha i}$-coupled receptor, an agonist inhibits the forskolin-induced cAMP production, resulting in an increase of the LANCE signal. On the other hand, an antagonist or inverse agonist decreases the LANCE signal toward forskolin-induced cAMP accumulation. Therefore, the detected LANCE signal is inversely proportional to cAMP level. As shown in Figure 4, reduction of the LANCE signal occurred with increasing concentrations of compounds **9, 18, 26, 27, 30, 59**; and **1**. These ligands acted as inverse agonists, indicated by increasing forskolin-induced cAMP production, with EC_{50} values of 159.1 ± 8.68,4.11 ± 3.66, 5.73 ± 6.37, 28.33 ± 2.54, 17.08 ± 2.1nM, 13.42 ± 2.07, and 13.71 ± 2.81 nM, respectively. Such a phenomenon was not observed with agonsits CP55940 and HU308, which inhibited cAMP production with EC_{50} values of 23.29 ± 4.17 and 83.81 ± 5.63 nM, respectively. The results clearly indicated that six compounds (**9, 18, 26, 27, 30**, and **59**) indeed behaved as inverse agonists.

NIH-PA Author Manuscript

NIH-PA Author Manuscript

NIH-PA Author Manuscript

Osteoclast Formation Bioactivity

On the basis of binding affinity, selectivity, functionality, and druglikeness studies above, four compounds were selected as top candidates for further biological study. As shown in Figure 5A, we tested the effect of these most promising CB_2 ligands on osteoclast (OCL) formation using human nonadherent mononuclear bone marrow cells.[37] Each ligand tested induced a concentration-dependent inhibition of osteoclastogenesis. Compared with the known CB_2 inverse agonist **1**, our compounds exhibited the same or stronger potency in suppressing OCL formation. Especially, compound **26** showed the strongest inhibition activity, with inhibition rates of 72%, 79% and 84% at 0.1, 1, and 10 μM, respectively. Importantly, **26** showed a more potent inhibitory effect than the parent ligand Xie95 (compound **9**), suggesting that our medicinal chemistry modification and SAR studies of Xie95 led to overall improved compounds not only for CB_2 activity but also for osteoclastogenesis inhibition.

Cytotoxicity Studies Using Normal Human Cells

Our newly discovered compounds showed promising inhibition activity with respect to osteoclastogenesis. To examine whether the impaired osteoclastogenesis in the presence of PAM compounds is due to their cell toxicity, we investigated the cytotoxicity profile of PAM compounds on normal human cells. First, mononuclear cells were isolated from healthy donors. After treatment of these normal cells with the PAM compounds for 3 days, the results indicated that the cell viability was not significantly affected in comparing with the vehicle control group (Figure 5B). The best compound **26** did not show any cytotoxic effects at the concentration (1 μM) of 79% inhibition of osteoclastogenesis, and only slight effects on cell viability were observed at high concentration of 10 μM. These results indicate that our compounds possess favorable therapeutic indexes and the inhibition of human osteoclastogenesis is not a result of their cytotoxicity.

QSAR Pharmacophore Modeling Studies of the New CB_2 Ligands

To compare the theoretical SAR models and activity data for further SAR study, 3D QSAR studies were carried out for the PAM analogues to generate CB_2 CoMFA SAR models by using our published protocol.[38,39] Given its high CB_2 affinity, selectivity, and strongest inhibition of osteoclastogenesis, compound **26** was selected as a template compound in our CoMFA studies. To search for preferred conformations of compound **26**, molecular dynamic simulations and molecular mechanics (MD/MM) were carried out based on our established computational protocol.[40] As described in the Experimental Section, MD simulations were performed with time steps of 1 fs for 300 ps with 1 ps interval recording time, which resulted in 300 conformers sampled after the simulations. All 300 conformations were minimized and converged to four families. Among four representative MD-generated conformers, one conformer had the conformation most similar to the docking pose that resulted from the molecular docking simulation (data not shown) using our refined 3D CB_2 receptor model.[41] The conformer was then chosen as one of the preferred active templates, and then all compounds from the training and test data sets were aligned to such preferred conformer of compound **26**. The final alignments of each set are depicted in Figure 6A,B.

After molecular alignment, leave-one-out cross-validation (LOOCV) analysis was performed to determine the optimal number of components and to evaluate the predictive ability of the derived CoMFA model which was measured by a cross-validated r^2 (r_{cv}^2). It is defined as

$$r_{\mathrm{CV}}{}^2 = (\mathrm{SD} - \mathrm{PRESS})/\mathrm{SD}$$

NIH-PA Author Manuscript

NIH-PA Author Manuscript

NIH-PA Author Manuscript

where SD is the sum of the squared deviations of each biological property value from their mean and PRESS is the sum, over all compounds, of the squared differences between the actual and predicted biological activity values. The LOOCV analysis showed that the optimal number of components was 4 and the r_{cv}^2 was 0.52, which was within the range of the generally accepted criterion for statistical validity.

Subsequently, non-cross-validated PLS analysis was performed and an r^2 of 0.924 with a standard error of estimate of 0.28 was obtained. Such a result indicates that the trained CoMFA model correlates well between PAM analogue structures and their CB_2 receptor affinity values. In order to evaluate the derived CoMFA model's generalization ability, it was used to predict the CB_2 binding activity values of test set compounds that were separated from the training set and hence were not included during the model training. A good correlation coefficient (r^2) of 0.76 was obtained from such prediction, and the result demonstrated that the CoMFA model had a good generalization performance on the test set compounds. As shown in Table 6, the predicted pK_i values are close to the experimental pK_i values for molecules in both training and test sets. Figure 7 shows the relationship between the calculated and experimental pK_i values for the non-cross-validated training set predictions and for the test set predictions. The linearity of the plot indicates a very good correlation and the ability of the developed CoMFA model to predict CB_2 receptor binding affinities of PAM derivatives.

To further predict favorable and unfavorable regions of PAM derivatives for CB_2 receptor binding activity, CoMFA contour maps were derived. In particular, CoMFA contour maps depict the color-coded electrostatic and steric regions around the molecules that associate with ligand biological activities. Green regions indicate favorable steric interactions that enhance binding affinity, whereas yellow regions display unfavorable steric interactions. On the other hand, the blue and red regions show preferred and not-preferred electrostatic interactions, respectively. As shown in Figure 6C, there is a sterically preferred region near the *p*-dimethylamino group, which means the hydrophobic pharmacophore feature in this part of the molecule is expected to enhance CB_2 receptor binding affinity. In fact, such a hydrophobic moiety may interact and fit well in the previously suggested hydrophobic pocket within transmembrane regions 3, 5, 6, and 7.[36,42–44] Moreover, this finding is consistent with our previous CoMFA studies,[39] which showed that the presence of a steric bulky group enhanced the CB_2 receptor binding activity and selectivity. On the other hand, electrostatic interactions are not preferred near the *p*-dimethylamino group as highlighted by a red region. This is congruent with the chemistry modifications of compounds **25** and **40** with *p*-NH_2 and *p*-NO_2 groups, respectively, which lost CB_2 binding activity. Once a hydrophobic feature was reintroduced, however, the CB_2 affinity and selectivity were restored, as demonstrated by compounds **17, 18, 21, 26, 27, 28, 29, 30**, and **31**. Therefore, our CoMFA studies corroborate our SAR hypothesis that aromatic ring C plays an important role in CB_2 receptor binding activity and introducing a hydrophobic feature at the para position of ring C is expected to enhance CB_2 receptor activity and selectivity.

CONCLUSION

We reported PAM as a novel chemotype with selective CB_2 receptor binding activity. In our SAR studies we have synthesized 52 new PAM derivatives designed through variations of the aromatic rings A–C and the substituents of different positions on these three rings. The SAR analyses reveal that (i) the para-substituted amino group on ring C plays a significant role in CB_2 receptor binding activity, a variety of functional groups was tolerated, and the *p*-dipropylamino group is optimal, (ii) *p*-Cl is a much better substituent than CF_3 and H on rings A and B, and aromatic rings A and B may be replaced by alkyl chains with the pentyl group being optimal, and (iii) aromatic ring C is an essential element to retain compound

NIH-PA Author Manuscript

NIH-PA Author Manuscript

NIH-PA Author Manuscript

potency to CB_2. Among the derivatives, five compounds **18, 26, 27, 30**, and **59** were confirmed as CB_2 inverse agonists with the strongest CB_2 receptor binding affinity and best selectivity. SAR pharmacophoric studies also confirmed our SAR findings that aromatic ring C is important for CB_2 receptor activity and a hydrophobic feature at the ring C's para position is crucial to improve CB_2 activity and selectivity of the PAM analogues. The results were congruent by chemistry, bioassay validation, and computer modeling studies. More importantly, osteoclastogenesis assay indicated that PAM compounds have promising inhibition activity to osteoclast cells derived human bone marrow. The most promising compound, **26**, showed 72% inhibition activity even at the low concentration of 0.1 μM. The inhibition of human osteoclastogenesis is not due to cytotoxic effects. Therefore, these PAM derivatives could be used as potential leads for the development of a new type of antiosteoporosis agent. Overall, the data presented here show that PAM is a new scaffold different from the existing CB_2 ligands and is promising for the design of new selective CB_2 receptor inverse agonists for further CB_2 signaling and antiosteoclast studies.

EXPERIMENTAL SECTION

Pharmacophore Modeling and Virtual Screening

A genetic algorithm-based pharmacophore alignment (GALAHAD) approach[32,33] was used to derive a 3D pharmacophore model based on known CB_2 antagonists including **1, 2, 3**, and **4** (Figure 2). The pharmacophore model was then examined and refined using our in-house training database which contained a mixture of decoy molecules and known CB2 ligands. The derived pharmacophore model was subsequently used as a query in the UNITY program[33] to perform virtual screening on a structurally diverse representative compound database.[34] Top ranked screened compounds from the pharmacophore search were obtained commercially or via material transfer agreement (MTA) to be experimentally validated for CB_2 binding activity and selectivity.

Chemistry

All reagents were purchased from commercial sources and used without further purification. Analytical thin-layer chromatography (TLC) was performed on SiO_2 plates on alumina. Visualization was accomplished by UV irradiation at 254 nm. Preparative TLC was conducted using preparative silica gel TLC plates (1000 μm, 20 cm × 20 cm). Flash column chromatography was performed using the Biotage Isolera flash purification system with SiO_2 60 (particle size 0.040–0.055 mm, 230–400 mesh). ^{1}H NMR was recorded on a Bruker 400 MHz spectrometer. Splitting patterns are indicated as follows: s, singlet; d, doublet; t, triplet; m, multiplet; br, broad peak. Purity of all final derivatives for biological testing was confirmed to be >95% as determined using the following conditions: a Shimadzu HPLC instrument with a Hamilton reversed phase column (HxSil, C18, 3 μm, 2.1 mm × 50 mm (H2)); eluent A consisting of 5% CH_3CN in H_2O; eluent B consisting of 90% CH_3CN in H_2O; flow rate of 0.2 mL/ min; UV detection, 254 and 214 nm.

General Procedure for Synthesis of 2-Phenylacetamide Building Blocks

2-Phenylacetamide—Benzyl cyanide (5 g, 42.7 mmol) was added slowly to concentrated sulfuric acid (20 mL) cooled by a water–ice bath. The solution was stirred overnight. The reaction mixture was poured into ice–water and neutralized with 20% NaOH. The aqueous phase was extracted by ethyl acetate (3 × 15 mL). The combined organic layer was washed with water (3 × 10 mL) and brine (3 × 10 mL), dried over anhydrous $MgSO_4$, filtered, concentrated under reduced pressure, and the residue was recrystallized from ethyl acetate and hexane to give the title compound (4.5 g, 78%). ^{1}H NMR (400 MHz, DMSO-d_6) δ 7.54 (s, 1H), 7.20–7.32 (m, 5H), 6.87 (s, 1H), 3.38 (s, 2H).

NIH-PA Author Manuscript

NIH-PA Author Manuscript

NIH-PA Author Manuscript

2-(4-Chlorophenyl)acetamide—^{1}H NMR (400 MHz, DMSO-d_6) δ 7.49 (s, 1H), 7.34–7.35 (m, 2H), 7.26–7.27 (m, 2H), 6.92 (s, 1H), 3.34–3.37 (m, 2H).

(4-(Trifluoromethyl)phenyl)acetamide —^{1}H NMR (400 MHz, DMSO-d_6) δ 7.65 (d, *J* = 8.0 Hz, 2H), 7.58 (s, 1H), 7.49 (d, *J* = 8.0 Hz, 2H), 7.00 (s, 1H), 3.51 (s, 2H).

General Procedure for the Coupling Reaction between Amide and Aldehyde

General Method 1

N,N′-((4-(*Dimethylamino)phenyl)methylene)bis(2-phenylacetamide*) (9): To a suspension of 4-(dimethylamino)benzaldehyde (149 mg, 1 mmol) and 2-phenylacetamide (270 mg, 2 mmol) in anhydrous dichloroethane (2 mL) was added TMSCl (216 mg, 2 mmol).[45] The mixture was heated at 70 °C for 12 h, then cooled to room temperature and the crude product precipitated from the solution. The crude product was recrystallized with methanol and hexane to give the final product (140 mg, 35%). ^{1}H NMR (400 MHz, DMSO-d_6) δ 8.89 (d, *J* = 8.0 Hz, 2H), 7.59 (s, 2H), 7.41 (d, *J* = 8.8 Hz, 2H), 7.21–7.32 (m, 10H), 6.54 (t, *J* = 8.0 Hz, 1H), 3.52 (dd, *J* = 14.0, 15.6 Hz, 4H), 3.06 (s, 6H). LC–MS (ESI): *m/z* 402.1 (M + H)$^+$. HRMS (ESI) for $C_{25}H_{28}N_3O_2$ (MH$^+$): calcd, 402.2176; found, 402.2179.

N,N′-(Phenylmethylene)bis(2-phenylacetamide) (11): Compound **11** was prepared from 2-phenylacetamide and benzaldehyde using method1. Yield: 67%. ^{1}H NMR (400 MHz, DMSO-d_6)δ 8.78 (d, *J* = 7.2 Hz, 2H), 7.21–7.35 (m, 15H), 6.55 (t, *J* = 7.8 Hz, 1H), 3.50 (dd, *J* = 13.8, 20.4 Hz, 4H). LC–MS (ESI): *m/z* 359.3 (M + H)$^+$.

N,N′-((2-Fluorophenyl)methylene)bis(2-phenylacetamide) (12): Compound **12** was prepared from 2-phenylacetamide and 2-fluorobenzaldehyde using method 1. Yield: 64%. ^{1}H NMR (400 MHz, DMSO-d_6) δ 8.87 (d, *J* = 7.8 Hz, 2H), 7.44 (t, *J* = 7.8 Hz, 1H), 7.36 (q, *J* = 6.6 Hz, 1H), 7.17–7.29 (m, 12H), 6.74 (t, *J* = 7.8 Hz, 1H), 3.48 (dd, *J* = 14.4, 24.0 Hz, 4H). LC–MS (ESI): *m/z* 377.2 (M + H)$^+$.

N,N′-((4-Fluorophenyl)methylene)bis(2-phenylacetamide) (14): Compound **14** was prepared from 2-phenylacetamide and 4-fluorobenzaldehyde using method 1.Yield: 72%. ^{1}H NMR (400 MHz, DMSO-d_6) δ 8.79 (d, *J* = 8.0 Hz, 2H), 7.16–7.36 (m, 14H), 6.54 (t, *J* = 8.0 Hz, 1H), 3.52 (dd, *J* = 14.4, 15.6 Hz, 4H). LC–MS (ESI): *m/z* 377.2 (M + H)$^+$.

N,N′-((4-Chlorophenyl)methylene)bis(2-phenylacetamide) (15): Compound **15** was prepared from 2-phenylacetamide and 4-chlorobenzaldehyde using method 1. Yield: 71%. ^{1}H NMR (400 MHz, DMSO-d_6) δ 8.83 (d, *J* = 7.8 Hz, 2H), 7.41 (d, *J* = 7.8 Hz, 2H), 7.21–7.32 (m, 12H), 6.51 (t, *J* = 7.8 Hz, 1H), 3.50 (dd, *J* = 14.4, 17.4 Hz, 4H). LC–MS (ESI): *m/z* 393.2 (M + H)$^+$.

N,N′-(p-Tolylmethylene)bis(2-phenylacetamide) (17): Compound **17** was prepared from 2-phenylacetamide and 4-methylbenzaldehyde using method 1.Yield: 70%. ^{1}H NMR (400 MHz, DMSO-d_6) δ8.71 (d, *J* = 8.0 Hz, 2H), 7.13–7.32 (m, 14H), 6.52 (t, *J* = 8.0 Hz, 1H), 3.51 (dd, *J* = 14.4, 15.6 Hz, 4H), 2.29 (S, 3H). LC–MS (ESI): *m/z* 373.1 (M +H)$^+$.

N,N′-((4-Methoxyphenyl)methylene)bis(2-phenylacetamide) (19): Compound **19** was prepared from 2-phenylacetamide and 4-methoxybenzaldehyde using method 1. Yield: 62%. ^{1}H NMR (400 MHz, DMSO-d_6) δ 8.70 (d, *J* = 7.6 Hz, 2H), 7.21–7.31 (m, 12H), 6.89 (d, *J* = 8.8 Hz, 2H), 6.51 (t, *J* = 8.0 Hz, 1H), 3.74 (s, 3H), 3.50 (dd, *J* = 14.0, 17.2 Hz, 4H). LC–MS (ESI): *m/z* 389.1 (M + H)$^+$.

NIH-PA Author Manuscript

NIH-PA Author Manuscript

NIH-PA Author Manuscript

N,N′-((2-(Trifluoromethyl)phenyl)methylene)bis(2-phenylaceta-mide)(22): Compound **22** was prepared from 2-phenylacetamide and 2-(trifluoromethyl)benzaldehyde using method 1. Yield: 70%. ^{1}H NMR (400 MHz, DMSO-d_6) δ 8.87 (d, *J* = 7.2 Hz, 2H), 7.78 (d, *J* = 7.6 Hz, 1H), 7.68–7.73 (m, 2H), 7.54 (t, *J* = 7.6 Hz, 1H), 7.19–7.30 (m, 10H), 6.83 (t, *J* = 6.8 Hz, 1H), 3.46 (dd, *J* = 14.0, 17.6 Hz, 4H). LC–MS (ESI): *m/z* 427.0 (M + H)$^+$.

N,N′-((4-(Trifluoromethyl)phenyl)methylene)bis(2-phenylaceta-mide)(23): Compound **23** was prepared from 2-phenylacetamide and 4-(trifluoromethyl)benzaldehyde using method 1. Yield: 75%. ^{1}H NMR (400 MHz, DMSO-d_6) δ 8.89 (d, *J* = 7.6 Hz, 2H), 7.72 (d, *J* = 7.6 Hz, 2H), 7.51 (d, *J* = 7.6 Hz, 2H), 7.25–7.30 (m, 10H), 6.58 (t, *J* = 7.2 Hz, 1H), 3.53 (s, 4H). LC–MS (ESI): *m/z* 427.2 (M + H)$^+$.

N,N′-((4-Nitrophenyl)methylene)bis(2-phenylacetamide)(24): Compound **24** was prepared from 2-phenylacetamide and 4-nitro-benzaldehyde using method 1. Yield: 84%. ^{1}H NMR (400 MHz, DMSO-d_6) δ 8.98 (d, *J* = 7.6 Hz, 2H), 8.20–8.23 (m, 2H), 7.56 (d, *J* = 8.4 Hz, 2H), 7.23–7.32 (m, 10H), 6.58 (t, *J* = 7.6 Hz, 1H), 3.53 (s, 4H). LC–MS (ESI): *m/z* 404.1 (M + H)$^+$.

N,N′-((4-(Dipropylamino)phenyl)methylene)bis(2-phenylaceta-mide)(27): Compound **27** was prepared from 2-phenylacetamide and 4-(dipropylamino)benzaldehyde using method 1. Yield: 15%. ^{1}H NMR (400 MHz, CD_3OD) δ 7.25–7.30 (m, 10H), 7.10 (d, *J* = 8.8 Hz, 2H), 6.62 (d, *J* = 8.8 Hz, 2H), 6.57 (s, 1H), 3.56 (s, 4H), 3.24–3.26 (m, 4H), 1.54–1.64 (m, 4H), 0.93 (t, *J* = 7.6 Hz, 6H). LC-MS (ESI): *m/z* 458.2 (M + H)$^+$. HRMS (ESI) for $C_{29}H_{36}N_3O_2$ (MH$^+$): calcd, 458.2802; found, 458.2792.

N,N′-((4-(Pyrrolidin-1-yl)phenyl)methylene)bis(2-phenylaceta-mide)(30): Compound **30** was prepared from 2-phenylacetamide and 4-(pyrrolidin-1-yl)benzaldehyde using method 1. Yield: 12%. ^{1}H NMR (400 MHz, DMSO-d_6) δ 8.58 (d, *J* = 8.0 Hz, 2H), 7.20–7.31 (m, 10H), 7.08 (d, *J* = 8.4 Hz, 2H), 6.42–6.49 (m, 3H), 3.44–3.45 (m, 4H), 3.18– 3.20 (m, 4H), 1.93–1.96 (m, 4H). LC–MS (ESI): *m/z* 428.2 (M +H)$^+$. HRMS (ESI) for $C_{27}H_{30}N_3O_2$ (MH$^+$): calcd, 428.2333; found, 428.2328.

N,N′-(Phenylmethylene)bis(2-(4-chlorophenyl)acetamide)(32): Compound **32** was prepared from 2-(4-chlorophenyl)acetamide and benzaldehyde using method 1. Yield: 52%. ^{1}H NMR (400 MHz, DMSO-d_6) δ 8.88 (d, *J* = 7.8 Hz, 2H), 7.25–7.41 (m, 13H), 6.52 (t, *J* = 7.8 Hz, 1H), 3.50 (s, 4H). LC–MS (ESI): *m/z* 427.1 (M + H)$^+$.

N,N′-((2-Fluorophenyl)methylene)bis(2-(4-chlorophenyl)-acetamide)(33): Compound **33** was prepared from 2-(4-chlorophenyl)acetamide and 2-fluorobenzaldehyde using method 1. Yield: 63%. ^{1}H NMR (400 MHz, DMSO-d_6) δ 8.93 (d, *J* = 7.2 Hz, 2H), 7.45 (t, *J* = 7.2 Hz, 1H), 7.33–7.37 (m, 5H), 7.25–7.26 (m, 4H), 7.18– 7.21 (m, 2H), 6.73 (t, *J* = 7.2 Hz, 1H), 3.48 (s, 4H). LC–MS (ESI): *m/z* 445.0 (M + H)$^+$.

N,N′-((4-Fluorophenyl)methylene)bis(2-(4-chlorophenyl)-acetamide)(34): Compound **34** was prepared from 2-(4-chlorophenyl)acetamide and 4-fluorobenzaldehyde using method 1. Yield: 67%. ^{1}H NMR (400 MHz, DMSO-d_6) δ 8.82 (d, *J* = 7.6 Hz, 2H), 7.34–7.37 (m, 6H), 7.27 (d, *J* = 8.4 Hz, 4H), 7.19 (t, *J* = 8.8 Hz, 2H), 6.51 (t, *J* = 8.0 Hz, 1H), 3.51 (s, 4H). LC–MS (ESI): *m/z* 444.9 (M + H)$^+$.

N,N′-((4-Chlorophenyl)methylene)bis(2-(4-chlorophenyl)-acetamide)(35): Compound **35** was prepared from 2-(4-chlorophenyl)acetamide and 4-chlorobenzaldehyde using method 1. Yield: 70%. ^{1}H NMR (400 MHz, DMSO-d_6) δ 8.88 (d, *J* = 7.8 Hz, 2H), 7.42 (d, *J* = 8.4 Hz,

NIH-PA Author Manuscript

NIH-PA Author Manuscript

NIH-PA Author Manuscript

2H), 7.31–7.35 (m, 6H), 7.26 (d, *J* = 8.4 Hz, 4H), 6.47 (t, *J* = 7.8 Hz, 1H), 3.50 (s, 4H). LC–MS (ESI): *m/z* 460.8 $(M + H)^+$.

N,N′-(p-Tolylmethylene)bis(2-(4-chlorophenyl)acetamide)(36): Compound **36** was prepared from 2-(4-chlorophenyl)acetamide and 4-methylbenzaldehyde using method 1. Yield: 88%. ^{1}H NMR (400 MHz, DMSO-d_6) δ 8.76 (d, *J* = 8.0 Hz, 2H), 7.34 (d, *J* = 8.4 Hz, 4H), 7.28 (d, *J* = 8.4 Hz, 4H), 7.17 (q, *J* = 8.0 Hz, 4H), 6.50 (t, *J* = 7.6 Hz, 1H), 3.51 (s, 4H), 2.29 (s, 3H). LC–MS (ESI): *m/z* 441.3 $(M + H)^+$.

N,N′-((4-Methoxyphenyl)methylene)bis(2-(4-chlorophenyl)-acetamide)(37): Compound **37** was prepared from 2-(4-chlorophenyl)acetamide and 4-methoxybenzaldehyde using method 1. Yield: 91%. ^{1}H NMR (400 MHz, DMSO-d_6) δ 8.73 (d, *J* = 7.6 Hz, 2H), 7.34 (d, *J* = 8.8 Hz, 4H), 7.26 (d, *J* = 8.4 Hz, 4H), 7.21 (d, *J* = 8.8 Hz, 2H), 6.90 (d, *J* = 8.8 Hz, 2H), 6.46 (t, *J* = 8.0 Hz, 1H), 3.74 (s, 3H), 3.49 (s, 4H). LC-MS (ESI): *m/z* 457.2 $(M + H)^+$.

N,N′-((2-(Trifluoromethyl)phenyl)methylene)bis(2-(4-chlorophenyl)acetamide)(38): Compound **38** was prepared from 2-(4-chlorophenyl)acetamide and 2-(trifluoromethyl)benzaldehyde using method 1. Yield: 82%.^{1}H NMR (400 MHz, DMSO-d_6) δ 8.04 (d,*J* = 6.0 Hz, 2H), 7.81 (d, *J* = 7.8 Hz, 1H), 7.72 (d, *J* = 7.8 Hz, 1H), 7.62 (t, *J* = 7.8 Hz, 1H), 7.52 (t, *J* = 7.8 Hz, 1H), 7.27–7.30 (m, 8H), 7.06 (t, *J* = 7.2 Hz, 1H), 3.52 (s, 4H). LC–MS (ESI): *m/z* 495.0 $(M + H)^+$.

N,N′-((4-(Trifluoromethyl)phenyl)methylene)bis(2-(4-chlorophenyl)acetamide)(39): Compound **39** was prepared from 2-(4-chlorophenyl)acetamide and 4-(trifluoromethyl)benzaldehyde using method 1. Yield: 85%.^{1}H NMR (400 MHz, DMSO-d_6) δ 8.96 (d,*J* = 7.6 Hz, 2H), 7.73 (d, *J* = 8.4 Hz, 2H), 7.54 (d, *J* = 8.4 Hz, 2H), 7.35 (d, *J* = 8.4 Hz, 4H), 7.28 (d, *J* = 8.4 Hz, 4H), 6.57 (t, *J* = 7.6 Hz, 1H), 3.54 (s, 4H). LC–MS (ESI): *m/z* 495.2 $(M + H)^+$.

N,N′-((4-Nitrophenyl)methylene)bis(2-(4-chlorophenyl)-acetamide)(40): Compound **40** was prepared from 2-(4-chlorophenyl)acetamide and 4-nitrobenzaldehyde using method 1. Yield: 90%. ^{1}H NMR (400 MHz, DMSO-d_6) δ 9.02 (d, *J* = 8.0 Hz, 2H), 8.24–8.25 (m, 2H), 7.56–7.58 (m, 2H), 7.34–7.37 (m, 4H), 7.26–7.29 (m, 4H), 6.55 (t, *J* = 8.0 Hz, 1H), 3.53 (S, 4H). LC–MS (ESI): *m/z* 472.0 $(M + H)^+$.

N,N′-(Phenylmethylene)bis(2-(4-(trifluoromethyl)phenyl)-acetamide)(41): Compound **41** was prepared from 2-(4-(trifluoromethyl)phenyl)acetamide and benzaldehyde using method 1. Yield: 83%. ^{1}H NMR (400 MHz, DMSO-d_6) δ 8.94 (d, *J* = 7.8 Hz, 2H), 7.63 (d, *J* = 7.8 Hz, 4H), 7.48 (d, *J* = 8.4 Hz, 4H), 7.29–7.37 (m, 5H), 6.55 (t, *J* = 7.8 Hz, 1H), 3.63 (s, 4H). LC–MS (ESI): *m/z* 495.1 $(M + H)^+$.

N,N′-((2-Fluorophenyl)methylene)bis(2-(4-(trifluoromethyl)-phenyl)acetamide)(42): Compound **42** was prepared from 2-(4-(trifluoromethyl)phenyl)acetamide and 2-fluorobenzaldehyde using method 1. Yield: 86%. ^{1}H NMR (400 MHz, DMSO-d_6) δ 8.99 (d, *J* = 7.2 Hz, 2H), 7.63 (d, *J* = 7.8 Hz, 4H), 7.46 (d, *J* = 7.8 Hz, 5H), 7.36–7.40 (m, 1H), 7.21 (t, *J* = 7.8 Hz, 2H), 6.74 (t, *J* = 7.8 Hz, 1H), 3.60 (s, 4H). LC–MS (ESI): *m/z* 513.0 $(M + H)^+$.

N,N′-((4-Fluorophenyl)methylene)bis(2-(4-(trifluoromethyl)-phenyl)acetamide)(43): Compound **43** was prepared from 2-(4-(trifluoromethyl)phenyl)acetamide and 4-fluorobenzaldehyde using method 1. Yield: 90%. ^{1}H NMR (400 MHz, DMSO-d_6) δ 8.95 (d, *J* = 8.4 Hz, 2H), 7.63 (d, *J* = 8.4 Hz, 4H), 7.47 d, *J* = 8.4 Hz, 4H), 7.37 (dd, *J* = 5.4, 8.4 Hz,

NIH-PA Author Manuscript

NIH-PA Author Manuscript

NIH-PA Author Manuscript

2H), 7.19 (t, *J* = 8.4 Hz, 2H), 6.51 (t, *J* = 7.8 Hz, 1H), 3.62 (s, 4H). LC–MS (ESI): *m/z* 513.2 $(M + H)^+$.

N,N′-((4-Chlorophenyl)methylene)bis(2-(4-(trifluoromethyl)-phenyl)acetamide)(44): Compound **44** was prepared from 2-(4-(trifluoromethyl)phenyl)acetamide and 4-chlorobenzaldehyde using method 1. Yield: 85%. ^{1}H NMR (400 MHz, DMSO-d_6) δ 8.96 (d,*J* = 7.8 Hz, 2H), 7.63 (d, *J* = 7.2 Hz, 4H), 7.46 (d, *J* = 7.8 Hz, 4H), 7.43 (dd, *J* = 1.8, 8.4 Hz, 2H), 7.34–7.35 (m, 2H), 6.50 (t, *J* = 7.2 Hz, 1H), 3.62 (s, 4H). LC–MS (ESI): *m/z* 529.0 $(M + H)^+$.

N,N′-(p-Tolylmethylene)bis(2-(4-(trifluoromethyl)phenyl)-acetamide)(45): Compound **45** was prepared from 2-(4-(trifluoromethyl)phenyl)acetamide and 4-methylbenzaldehyde using method 1. Yield: 81%. ^{1}H NMR (400 MHz, DMSO-d_6) δ 8.87 (d,*J* = 8.4 Hz, 2H), 7.63 (d, *J* = 7.8 Hz, 4H), 7.47 (d, *J* = 8.4 Hz, 4H), 7.20 (d, *J* = 8.4 Hz, 2H), 7.15 (d, *J* = 7.8 Hz, 2H), 6.49 (t, *J* = 7.8 Hz, 1H), 3.61 (s, 4H), 2.28 (s, 3H). LC–MS (ESI): *m/z* 509.1 $(M + H)^+$.

N,N′-((4-Methoxyphenyl)methylene)bis(2-(4-(trifluoromethyl)-phenyl)acetamide)(46): Compound **46** was prepared from 2-(4-(trifluoromethyl)phenyl)acetamide and 4-methoxybenzaldehyde using method 1. Yield: 86%. ^{1}H NMR (400 MHz, DMSO-d_6) δ 8.85 (d, *J* = 7.8 Hz, 2H), 7.63 (d, *J* = 7.8 Hz, 4H), 7.47 (d, *J* = 7.8 Hz, 4H),7.24 (d, *J* = 9.0 Hz, 2H), 6.91 (d, *J* = 8.4 Hz, 2H), 6.48 (t, *J* = 7.8 Hz, 1H), 3.74 (s, 3H), 3.61(s, 4H). LC–MS (ESI): *m/z* 525.1 $(M + H)^+$.

N,N′-((4-(Trifluoromethyl)phenyl)methylene)bis(2-(4-(trifluoromethyl)phenyl)acetamide)(47): Compound **47** was prepared from 2-(4-(trifluoromethyl)phenyl)acetamide and 4-(trifluoromethyl)-benzaldehyde using method 1. Yield: 74%. ^{1}H NMR (400 MHz, DMSO-d_6) δ 9.08 (d, *J* = 7.2 Hz, 2H), 7.73 (d, *J* = 7.8 Hz, 2H), 7.63 (d, *J* = 7.8 Hz, 4H), 7.56 (d, *J* = 7.8 Hz, 2H), 7.48 (d, *J* = 7.8 Hz, 4H), 6.60 (t, *J* = 7.8 Hz, 1H), 3.35–3.43 (m, 4H). LC–MS (ESI): *m/z* 562.9 $(M + H)^+$.

N,N′-((4-(Diethylamino)phenyl)methylene)dibenzamide (51): Compound **51** was prepared from benzamide and 4-(diethylamino)-benzaldehyde using method 1. Yield: 73%. ^{1}H NMR (400 MHz, CD_3OD) δ 9.24 (d, *J* = 7.6 Hz, 1H), 7.88–7.93 (m, 4H), 7.81 (d, *J* = 8.8 Hz, 2H), 7.46–7.65 (m, 9H), 7.20 (m, 1H), 3.70–3.81 (m, 4H), 1.17 (t, *J* = 7.2 Hz, 6H). LC–MS (ESI): *m/z* 402.2 $(M + H)^+$. HRMS (ESI) for $C_{25}H_{28}N_3O_2$ (MH^+): calcd, 402.2176; found, 402.2167.

N,N′-((4-(Diethylamino)phenyl)methylene)bis(3-phenylpropana-mide)(52): Compound **52** was prepared from 3-phenylpropanamide and 4-(diethylamino)benzaldehyde using method 1. Yield: 66%. ^{1}H NMR (400 MHz, CD_3OD) δ 8.29–8.30 (m, 2H), 7.17–7.29 (m, 10H), 6.92 (d, *J* = 8.4 Hz, 2H), 6.56 (d, *J* = 8.4 Hz, 2H), 6.46 (t, *J* = 8.0 Hz, 1H), 2.82 (t, *J* = 7.6 Hz, 4H), 2.42–2.47 (m, 4H), 1.07 (t, *J* = 6.8 Hz, 6H). LC–MS (ESI): *m/z* 458.2 $(M + H)^+$. HRMS (ESI) for $C_{29}H_{36}N_3O_2$ (MH^+): calcd, 458.2802; found, 458.2795.

N,N′-((4-(Diethylamino)phenyl)methylene)bis(3-phenylacryla-mide)(53): Compound **53** was prepared from cinnamamide and 4-(diethylamino)benzaldehyde using method 1. Yield: 68%. ^{1}H NMR (400 MHz, CD_3OD) δ 8.68–8.70 (m, 2H), 7.38–7.58 (m, 12H), 7.19 (d, *J* = 8.8 Hz, 2H), 6.79 (d, *J* = 16.0 Hz, 2H), 6.66–6.68 (m, 3H), 3.29–3.35 (m, 4H), 1.08 (t, *J* = 7.2 Hz, 6H). LC–MS (ESI): *m/z* 454.2 $(M + H)^+$. HRMS (ESI) for $C_{29}H_{32}N_3O_2$ (MH^+): calcd, 454.2489; found, 454.2487.

NIH-PA Author Manuscript

NIH-PA Author Manuscript

NIH-PA Author Manuscript

N,N′-((4-(Diethylamino)phenyl)methylene)bis(2-methylpropana-mide)(56): Compound **56** was prepared from isobutyramide and 4-(diethylamino)benzaldehyde using method 1. Yield: 80%. ^{1}H NMR (400 MHz, CD_3OD) δ 7.18 (d, *J* = 8.4 Hz, 2H), 6.70–6.73 (m, 2H), 6.56 (s, 1H), 3.35–3.50 (m, 2H), 2.47–2.54 (m, 4H), 1.13–1.16 (m, 12H). LC–MS (ESI): *m/z* 334.2 $(M + H)^+$. HRMS (ESI) for $C_{19}H_{32}N_3O_2$ (MH^+): calcd, 334.2489; found, 334.2483.

N,N′-((4-(Diethylamino)phenyl)methylene)bis(2,2-dimethylpro-panamide)(57): Compound **57** was prepared from pivalamide and 4-(diethylamino)benzaldehyde using method 1. Yield: 77%. ^{1}H NMR (400 MHz, DMSO) δ 7.70 (d, *J* = 8.8 Hz, 2H), 7.03 (d, *J* = 8.8 Hz, 2H), 6.62 (d, *J* = 8.8 Hz, 2H), 6.52 (t, *J* = 8.4 Hz, 1H), 3.30–3.33 (m, 4H), 1.12 (s, 18H), 1.05–1.08 (m, 6H). LC–MS (ESI): *m/z* 262.2 $(M + H)^+$. HRMS (ESI) for $C_{21}H_{36}N_3O_2$ (MH^+): calcd, 362.2802; found, 362.2795.

N,N′-((4-(Diethylamino)phenyl)methylene)dipentanamide (58): Compound **58** was prepared from pentanamide and 4-(diethylamino)-benzaldehyde using method 1. Yield: 69%. ^{1}H NMR (400 MHz, CD_3OD) δ 7.18 (d, *J* = 8.8 Hz, 2H), 6.71 (d, *J* = 8.8 Hz, 2H), 6.58 (t, *J* = 8.4 Hz, 1H), 3.33–3.41 (m, 4H), 2.25 (t, *J* = 7.2 Hz, 4H), 1.58–1.66 (m, 4H), 1.33–1.43 (m, 4H), 1.14 (t, *J* = 7.2 Hz, 6H), 0.95 (t, *J* = 2.8 Hz, 6H). LC–MS (ESI): *m/z* 362.2 $(M + H)^+$. HRMS (ESI) for $C_{21}H_{36}N_3O_2$ (MH^+): calcd, 362.2802; found, 362.2792.

N,N′-((4-(Diethylamino)phenyl)methylene)dihexanamide (59): Compound **59** was prepared from hexanamide and 4-(diethylamino)-benzaldehyde using method 1. Yield: 76%. ^{1}H NMR (400 MHz, CD_3OD) δ 7.19 (d, *J* = 8.8 Hz, 2H), 6.71 (d, *J* = 8.8 Hz, 2H), 6.58 (t, *J* = 8.4 Hz, 1H), 3.35–3.41 (m, 4H), 2.19–2.26 (m, 4H), 1.61–1.68 (m, 4H), 1.32–1.35 (m, 8H), 1.14 (t, *J* = 6.8 Hz, 6H), 0.94 (t, *J* = 2.8 Hz, 6H). LC–MS (ESI): *m/z* 390.3 $(M + H)^+$. HRMS (ESI) for $C_{23}H_{40}N_3O_2$ (MH^+): calcd, 390.3115; found, 390.3108.

N,N′-((4-(Diethylamino)phenyl)methylene)dioctanamide (60): Compound **60** was prepared from octanamide and 4-(diethylamino)-benzaldehyde using method 1. Yield: 68%. ^{1}H NMR (400 MHz, DMSO) δ 8.21 (d, *J* = 8.0 Hz, 2H), 7.07 (d, *J* = 8.8 Hz, 2H), 6.61 (d, *J* = 8.8 Hz, 2H), 6.42 (t, *J* = 8.0 Hz, 1H), 3.29–3.31 (m, 4H), 2.06–2.14 (m, 4H), 1.47–1.50 (m, 4H), 1.08–1.24 (m, 16H), 1.06 (t, *J* = 7.2 Hz, 6H), 0.94 (t, *J* = 7.2 Hz, 6H). LC–MS (ESI): *m/z* 446.3 $(M + H)^+$. HRMS (ESI) for $C_{27}H_{48}N_3O_2$ (MH^+): calcd, 446.3741; found, 446.3734.

N,N′-((4-(Diethylamino)phenyl)methylene)bis(decanamide)(61): Compound **61** was prepared from decanamide and 4-(diethylamino)-benzaldehyde using method 1. Yield: 56%. ^{1}H NMR (400 MHz, DMSO) δ 8.99 (d, *J* = 9.6 Hz, 1H), 8.38 (d, *J* = 8.8 Hz, 1H), 6.99 (d, *J* = 8.8 Hz, 2H), 6.58 (d, *J* = 8.4 Hz, 2H), 5.84 (d, *J* = 8.4 Hz, 1H), 3.27–3.30 (m, 4H), 2.33 (t, *J* = 7.2 Hz, 4H), 2.14 (t, *J* = 7.2 Hz, 4H), 1.50–1.55 (m, 4H), 1.24–1.28 (m, 24H), 1.06 (t, *J* = 7.2 Hz, 6H), 0.87 (t, *J* = 7.2 Hz, 6H). LC–MS (ESI): *m/z* 502.4 $(M + H)^+$.

General Method 2

N,N′-(2-Phenylethane-1,1-diyl)bis(2-phenyl-acetamide) (48): To a well stirred suspension of 2-phenylacetamide (540 mg, 4 mmol) in dry dichloromethane (2 mL) was added the 2-phenylacetaldehyde (240 mg, 2 mmol) and trimethylsilyltrifluoro-methane sulfonate (22 mg, 0.1 mmol).[46] The mixture was vigorously stirred for 12 h at room temperature, diluted with toluene (4 mL), and filtered. The precipitate was washed several times with toluene which was recrystallized with methanol and hexane to give the final product (560 mg, 76%). ^{1}H NMR (400 MHz, DMSO-d_6) δ 8.45 (d, *J* = 7.6 Hz, 2H), 7.14–7.28 (m, 15H), 5.55 (t, *J* = 7.6 Hz, 1H), 3.39 (s, 4H), 2.93 (d, *J* = 7.2 Hz, 2H). HPLC–MS (ESI): *m/z* 373.2 $(M + H)^+$.

NIH-PA Author Manuscript

NIH-PA Author Manuscript

NIH-PA Author Manuscript

N,N′-((3-Fluorophenyl)methylene)bis(2-phenylacetamide) (13): Compound **13** was prepared from 2-phenylacetamide and 3-fluorobenzaldehyde using method 2. Yield: 77%. ^{1}H NMR (400 MHz, DMSO-d_6) δ 8.83 (d, *J* = 8.0 Hz, 2H), 7.06–7.42 (m, 14H), 6.53 (t, *J* = 7.6 Hz, 1H), 3.47–3.55 (m, 4H). LC–MS (ESI): *m/z* 377.2 (M + H)$^+$.

N,N′-((4-Bromophenyl)methylene)bis(2-phenylacetamide) (16): Compound **16** was prepared from 2-phenylacetamide and 4-bromobenzaldehyde using method 2. Yield: 89%. ^{1}H NMR (400 MHz, DMSO-d_6) δ 8.82 (d, *J* = 7.6 Hz, 2H), 7.53–7.56 (m, 2H), 7.21–7.33 (m, 12H), 6.48 (t, *J* = 7.6 Hz, 1H), 3.46–3.54 (m, 4H). LC–MS (ESI): *m/z* 437.0 (M + H)$^+$.

N,N′-((4-Isopropylphenyl)methylene)bis(2-phenylacetamide)(18): Compound **18** was prepared from 2-phenylacetamide and 4-isopropylbenzaldehyde using method 2. Yield: 65%. ^{1}H NMR (400 MHz, DMSO-d_6) δ 8.73 (d, *J* = 8.0 Hz, 2H), 7.20–7.32 (m, 14H), 6.51 (t, *J* = 8.0 Hz, 1H), 3.46–3.54 (m, 4H), 2.85–2.89 (m, 1H), 1.19 (d, *J* = 6.8 Hz, 6H). LC–MS (ESI): *m/z* 401.2 (M + H)$^+$. HRMS (ESI) for $C_{26}H_{29}N_2O_2$ (MH$^+$): calcd, 401.2224; found, 401.2219.

N,N′-((4-Ethoxyphenyl)methylene)bis(2-phenylacetamide) (20): Compound **20** was prepared from 2-phenylacetamide and 4-ethoxybenzaldehyde using method 2. Yield: 70%. ^{1}H NMR (400 MHz, DMSO-d_6) δ 8.69 (d, *J* = 8.0 Hz, 2H), 7.18–7.31 (m, 10H), 6.88 (d, *J* = 6.4 Hz, 2H), 6.48 (t, *J* = 8.0 Hz, 1H), 3.98–4.03 (m, 2H), 3.45–3.52 (m, 4H), 1.31 (t, *J* = 6.8 Hz, 3H). LC–MS (ESI): *m/z* 403.1 (M + H)$^+$.

N,N′-((4-Isopropoxyphenyl)methylene)bis(2-phenylacetamide) (21): Compound **21** was prepared from 2-phenylacetamide and 4-isopropoxybenzaldehyde using method 2. Yield: 81%. ^{1}H NMR (400 MHz, DMSO-d_6) δ 8.69 (d, *J* = 7.6 Hz, 2H), 7.18–7.13 (m, 12H), 6.87 (d, *J* = 6.8 Hz, 2H), 6.48 (t, *J* = 8.0 Hz, 1H), 4.58–4.61 (m, 1H), 3.45–3.53 (m, 4H), 1.25 (d, *J* = 6.0 Hz, 6H). LC–MS (ESI): *m/z* 417.2 (M + H)$^+$.

N,N′-((4-(Diethylamino)phenyl)methylene)bis(2-phenylaceta-mide) (26): Compound **26** was prepared from 2-phenylacetamide and 4-(diethylamino)benzaldehyde using method 2. Yield: 78%. ^{1}H NMR (400 MHz, DMSO-d_6) δ 8.60 (d, *J* = 8.0 Hz, 2H), 7.21–7.31 (m, 10H), 7.07 (d, *J* = 8.4 Hz, 2H), 6.60 (d, *J* = 8.8 Hz, 2H), 6.43 (t, *J* = 8.0 Hz, 1H), 3,44–3.52 (m, 4H), 3.29–3.34 (m, 4H), 1.06 (t, *J* = 7.6 Hz, 6H). LC–MS (ESI): *m/z* 430.3 (M + H)$^+$. HRMS (ESI) for $C_{27}H_{32}N_3O_2$ (MH$^+$): calcd, 430.2489; found, 430.2496.

N,N′-((4-(Dibutylamino)phenyl)methylene)bis(2-phenylaceta-mide) (28): Compound **28** was prepared from 2-phenylacetamide and 4-(dibutylamino)benzaldehyde using method 2. Yield: 85%. ^{1}H NMR (400 MHz, DMSO-d_6) δ 8.58 (d, *J* = 8.0 Hz, 2H), 7.20–7.31 (m, 10H), 7.06 (d, *J* = 8.8 Hz, 2H), 6.57 (d, *J* = 8.8 Hz, 2H), 6.41 (t, *J* = 8.0 Hz, 1H), 3.47–3.48 (m, 4H), 3.22–3.26 (m, 4H), 1.43–1.50 (m, 4H), 1.26–1.35 (m, 4H), 0.91 (t, *J* = 7.6 Hz, 6H). LC–MS (ESI): *m/z* 486.2 (M + H)$^+$.

N,N′-((4-(Piperidin-1-yl)phenyl)methylene)bis(2-phenylaceta-mide)(31): Compound **31** was prepared from 2-phenylacetamide and 4- (piperidin-1-yl)benzaldehyde using method 2. Yield: 85%. ^{1}H NMR (400 MHz, DMSO-d_6) δ 8.80 (d, *J* = 8.0 Hz, 2H), 7.15–7.32 (m, 14H), 6.51 (t, *J* = 8.0 Hz, 1H), 3.37–3.52 (m, 8H), 1.61–1.83 (m, 6H). LC–MS (ESI): *m/z* 442.3 (M + H)$^+$.

N,N′-(3-Phenylpropane-1,1-diyl)bis(2-phenylacetamide) (49): Compound **49** was prepared from 2-phenylacetamide and 3-phenyl-propanal using method 2.Yield: 92%. ^{1}H

NIH-PA Author Manuscript

NIH-PA Author Manuscript

NIH-PA Author Manuscript

NMR (400 MHz, DMSO-d_6) δ 8.45 (d, *J* = 7.6 Hz, 2H), 7.10–7.31 (m, 15H), 5.26 (t, *J* = 7.6 Hz, 1H), 3.38–3.46 (m, 4H), 2.47–2.53 (m, 2H), 1.88–1.94 (m, 2H). LC–MS (ESI): *m/z* 387.3 $(M + H)^+$.

(E)-N,N′-(3-Phenylprop-2-ene-1,1-diyl)bis(2-phenylacetamide) (50): Compound **50** was prepared from 2-phenylacetamide and cinnamaldehyde using method 2. Yield: 88%. ^{1}H NMR (400 MHz, DMSO-d_6) δ 8.61 (d, *J* = 7.6 Hz, 2H), 7.21–7.37 (m, 15H), 6.41–6.45 (m, 1H), 6.27–6.32 (m, 1H), 6.04–6.09 (m, 1H), 3.44–3.52 (m, 4H). LC–MS (ESI): *m/z* 385.1 $(M + H)^+$.

N,N′-(Pentane-1,1-diyl)bis(2-phenylacetamide) (54): Compound **54** was prepared from 2-phenylacetamide and pentanal using method 2. Yield: 83%. ^{1}H NMR (400 MHz, DMSO-d_6) δ 8.25 (d, *J* = 8.0 Hz, 2H), 7.19–7.30 (m, 8H), 5.30 (t, *J* = 7.6 Hz, 1H), 3.36–3.44 (m, 4H), 1.56–1.62 (m, 2H), 1.14–1.26 (m, 4H), 0.81 (t, *J* = 7.2 Hz, 3H). LC–MS (ESI): *m/z* 339.1 $(M + H)^+$.

N,N′-(Hexane-1,1-diyl)bis(2-phenylacetamide) (55): Compound **55** was prepared from 2-phenylacetamide and hexanal using method 2. Yield: 93%. ^{1}H NMR (400 MHz, DMSO-d_6) δ 8.25 (d, *J* = 8.0 Hz, 2H), 7.19–7.30 (m, 8H), 5.29 (t, *J* = 7.6 Hz, 1H), 3.39–3.44 (m, 4H), 1.57–1.59 (m, 2H), 1.18–1.23 (m, 6H), 0.82 (t, *J* = 6.8 Hz, 3H). LC–MS (ESI): *m/z* 353.3 $(M + H)^+$.

General Method of Reduction

N,N′-((4-Aminophenyl)-methylene)bis(2-phenylacetamide) (25)—To a well stirred suspension of N,N′-((4-nitrophenyl)methylene)bis(2-phenylacetamide) (**24**) (403 mg, 1 mmol) in ethanol (2 mL) was added the palladium (10%, 3.0 mg) and hydrazine (0.05 mL, 1.5 mmol). The mixture was vigorously stirred for 3 h at 70 °C. After filtration, the filtrate was evaporated to dryness on a rotary evaporator. The crude compound was further purified by recrystallization from ethanol. After the sample was dried in a vacuum at room temperature, **25** was obtained as a yellow solid (370 mg, 99%). ^{1}H NMR (400 MHz, DMSO-d_6) δ 8.54 (d, *J* = 8.0 Hz, 2H), 7.20–7.31 (m, 10H), 6.92 (d, *J* = 8.4 Hz, 2H), 6.49 (d, *J* = 8.4 Hz, 2H), 6.39 (t, *J* = 8.0 Hz, 1H), 5.04 (bs, 2H), 3.43–3.53 (m, 4H). LC–MS (ESI): *m/z* 374.1 $(M + H)^+$.

General Method of Alkylation

N,N′-((4-(Dibenzylamino)-phenyl)methylene)bis(2-phenylacetamide) (29)— Compound **25** (373 mg, 1 mmol), K_2CO_3 (0.27 g, 1.95 mmol), and DMF (10 mL) were placed in a flask equipped with a condenser and a magnetic stirrer. Benzyl bromide (376 mg, 2.2 mmol) was added, and the mixture was stirred at room temperature for 12 h. The reaction solution was poured into water and extracted with EA. The combined organic layers were washed with water and brine and then dried over Na_2SO_4. The mixture was filtered, and the solvent was evaporated in vacuum. The residue was purified by flash chromatography on silica gel to obtain **29** (282 mg, 51%). ^{1}H NMR (400 MHz, DMSO-d_6) δ 8.50 (s, 2H), 7.18–7.35 (m, 20H), 7.01 (d, *J* = 8.8 Hz, 2H), 6.62 (d, *J* = 8.8 Hz, 2H), 6.39 (t, *J* = 8.0 Hz, 1H), 4.70 (s, 4H), 3.44–3.45 (m, 4H). LC–MS (ESI): *m/z* 554.2$(M + H)^+$.

Radioligand Competition Binding Assays

CB ligand competition binding assay was carried out as described previously.[31] Briefly, nonradioactive (or cold) ligands (PAM derivatives and reference ligands) were diluted in binding buffer (50 mM Tris-HCl (pH 7.4), 5 mM $MgCl_2$, 2.5 mM EGTA, and 0.1% (w/v) fatty acid free BSA), supplemented with 10% dimethyl sulfoxide and 0.4% methylcellulose.

NIH-PA Author Manuscript

NIH-PA Author Manuscript

NIH-PA Author Manuscript

Each assay plate well contained a total of 200 μL of reaction mixture comprising 5 μg of CB_1 (or CB_2) membrane protein, labeled [^{3}H]CP-55,940 ligand at a final concentration of 3 nM, and the unlabeled ligand at its varying dilutions as stated above. Plates were incubated at 30 °C for 1 h with gentle shaking. The reaction was terminated by rapid filtration through Unifilter GF/B filter plates using a UniFilter cell harvester (PerkinElmer). After the plate was allowed to dry overnight, 30 μL MicroScint-0 cocktail (PerkinElmer) was added to each well and the radioactivity was counted by using a PerkinElmer TopCount. All assays were performed in duplicate and data points represented as the mean ± SEM. Bound radioactivity data were analyzed for K_i values using nonlinear regression analysis via GraphPad Prism 5.0 software.

The saturation binding of [^{3}H]CP-55,940 to the membrane proteins was performed as described previously.[36] Briefly, the CB_1 (or CB_2) membrane fractions (5 (μg) were incubated with increasing concentrations of [^{3}H]CP-55,940 (0.05–4 nM) in 96-well plates at 30 °C with slow shaking for 1 h. The incubation buffer was composed of 50 mM Tris-HCl (pH 7.4), 5 mM $MgCl_2$, 2.5 mM EGTA, and 0.1% (w/v) fatty acid free BSA Ligand was diluted in incubation buffer supplemented with 10% dimethyl sulfoxide and 0.4% methylcellulose. Nonspecific binding was determined in the presence of unlabeled CP-55,940 (5000 nM). The reaction was terminated and the radioactivity was counted as stated above. Nonlinear regression analysis revealed the receptor density (B_{max}) and the equilibrium dissociation constant (K_d) of [^{3}H]CP-55,940 for the CB_2 receptor.

cAMP Assays

Cellular cAMP levels were measured according to a reported method with modifications using LANCE cAMP 384 kits (PerkinElmer).[36] The assay is based on competition between a europium-labeled cAMP trace complex and total cAMP for binding sites on cAMP-specific antibodies labeled with a fluorescent dye. The energy emitted from the Eu chelate is transferred to the dye on the antibodies, which in turn generates a time-resolved fluorescent resonant energy transfer (TR-FRET) signal at 665 nm. The fluorescence intensity (665 nm) decreases in the presence of cAMP from the tested samples, and resulting signals are inversely proportional to the cAMP concentration of a sample. CB_2 receptor wild type (WT) transfected CHO cells were seeded in a 384-well white ProxiPlates with a density of 2000 cells per well in 5 μL of RPMI-1640 medium containing 1% dialyzed FBS, 25 mM HEPES, 100 μg/mL pennicilin, 100 U/mL strepmicin, and 200 μg/mL G-418. After culture overnight, 2.5 μL of cAMP antibody and RO20-1724 (final consentration of 50 μM) in stimulation buffer (DPBS 1×, containing 0.1% BSA) was added to each well, followed by addition of either 2.5 μL compound or forskolin (final 5 μM) for agonist-inhibited adenylate cyclase (AC) activity assay. After incubated at room temperature for 45 min, 10 μL of detection reagent was added into each well. The plate was then incubated for 1 h at room temperature and measured in Synergy H1 hybrid reader (BioTek) with excitation at 340 nm and emission at 665 nm. Each cAMP determination was made via at least two independent experiments, each in triplicate. $EC5_0$ values were determined by nonlinear regression of dose-response curves (GraphPad Prism 5).

Osteoclast Formation Assay

Human marrow-derived mononuclear cells (2 × 10 cells/well) were seeded in 96-well multiplates at 100 μL/well in a MEM containing 20% horse serum, 10 ng/mL M-CSF, and 25 ng/mL RANKL. The tested compounds at the indicated final concentrations were added to the appropriate wells. Half-medium changes were carried out twice a week using drug-containing medium where appropriate. The culture was incubated for a total of 3 weeks at 37 °C with 5% CO_2 and 95% humidity. Differentiation into OCLs was assessed by staining with monoclonal antibody 23c6 using a Vectastatin-ABC-AP kit (Vector Laboratories,

NIH-PA Author Manuscript

NIH-PA Author Manuscript

NIH-PA Author Manuscript

Burlingame, CA). The antibody 23c6, which recognizes CD51/61 dimer constituting the OCL vitronectin receptor, was generously provided by Mchael Horton (Rayne Institute, Bone and Mineral Center, London, U.K.). The 23c6-positive multinucleated OCLs containing three or more nuclei per OCL were scored using an inverted microscope.[47]

Cytotoxicity Assay on Human Mononuclear Cells

Peripheral blood was drawn in a heparinized syringe from healthy fasting volunteers who had been without medication for at least 2 weeks. The peripheral blood mononuclear cell (PBMC) fraction was obtained by gradient centrifugation over Ficoll-Hypaque (Amersham), as described previously.[48] PBMC were washed three times with ice-cold PBS, followed by resuspension at 5×10^5/mL in the culture medium supplemented with 10% inactivated FBS, 2 mM glutamine, 100 U/mL penicillin, and 100 μg/mL streptomycin (Sigma). The compounds in a stock solution (50 mM in DMSO) were diluted with the culture medium to application conditions and further used for the treatment of PBMC for 3 days. The final DMSO concentrations are always 0.02%. After treatment for 72 h, cell viability was determined using trypan blue exclusion assay. These human cell studies conformed to the guidelines of the Institutional Review Board of the University of Pittsburgh, PA.

Molecular Modeling and CoMFA Studies

Out of the 52 compounds from Tables 1–5, 40 compounds were used in the subsequent 3D QSAR CoMFA studies. Twelve compounds that showed no binding, hence no experimental K_i, were ignored in the analysis. Approximately 75% (29 compounds) and 25% (11 compounds) were randomly selected as a training set and a test set, respectively. Molecular modeling and CoMFA studies were performed using the SYBYL X1.2 from the Tripos molecular modeling package.[49] By use of our established protocol, [38–40] molecular dynamic simulations were carried out for the best compound **26**. Briefly, dynamic simulations were simulated at 300 K with a time steps of 1 fs for a total duration of 300 ps, and conformation samples were collected at every 1 ps, resulting in 300 conformers of compound **26**. All conformers were then minimized and converged into four families. These four representative conformers derived from MD simulations were compared to the docking pose resulting from the molecular docking experiment using our in-house 3D CB_2 receptor model. The docking experiment was done using the Surflex-Dock module from the Tripos modeling software. The conformer with maximum agreement between these two experiments was chosen as a preferred conformer for further CoMFA studies. Structural alignments of all molecules in the training and test sets to the preferred conformer of compound **26** were performed using the MultiFit program in Sybyl X1.2. The CoMFA study was then carried out using the SYBYL/CoMFA module. The steric and electrostatic field energies (Gasteiger–Huckel charge) were calculated using the default parameters, namely, the Tripos standard CoMFA field class, distance-dependent dielectric constant, steric and electrostatic field cutoff set at 30 $kcal \cdot mol^{-1}$. Leave one-out cross-validation (LOOCV) partial least squares (PLS) analysis was then performed with a minium σ (column filter) value of 5.0 $kcal \cdot mol^{-1}$ to improve the signal-to-noise ratio by omitting those lattice points whose energy variation was below this threshold. The final model (non-cross-validated analysis) was developed from the LOOCV model with the highest cross-validated r^2, using the optimal number of components determined by the LOOCV model.

Acknowledgments

The authors gratefully acknowledge financial support from NIH Grant R01DA025612 (X.-Q.X.) and the National Natural Science Foundation of China (NSFC81090410, NSFC90913018). K.-Z.M. is a predoctoral trainee supported by NIH T32 Training Grant T32 EB009403 under the Joint CMU-Pitt computational biology Ph.D. program.

NIH-PA Author Manuscript

NIH-PA Author Manuscript

NIH-PA Author Manuscript

ABBREVIATIONS USED

CB	cannabinoid
AMTa	anandamide membrane transporter
FAAH	fatty acid amide hydrolase
MAGL	monoacylglycerol lipase
GPCR	G-protein-coupled receptor
GALAHAD	genetic algorithm-based pharmacophore alignment
CoMFA	comparative molecular field analysis
QSAR	quantitative structure-activity relationship
HB	H-bond
PAM	phenylacetamide
OCL	osteoclast
MD	molecular dynamics
MM	molecular mechanics
LOOCV	leave-one-out cross-validation
MTA	material transfer agreement
TLC	thin-layer chromatography
TMSCl	trimethylsilyl chloride
DMSO	dimethyl sulfoxide
DMF	dimethylformamide
EA	ethyl acetate
BSA	bovine serum albumin
EGTA	ethylene glycol tetraacetic acid
TR-FRET	time-resolved fluorescent resonant energy transfer
WT	wild type
FBS	fetal bovine serum
DPBS	Dulbecco's phosphate buffered saline
AC	adenylate cyclase
MEM	minimal essential medium
M-CSF	macrophage colony-stimulating factor
RANKL	receptor activator of nuclear factor κB ligand
PBMC	peripheral blood mononuclear cell
PLS	partial least squares

REFERENCES

1. Beltramo M, Stella N, Calignano A, Lin SY, Makriyannis A, Piomelli D. Functional role of high-affinity anandamide transport, as revealed by selective inhibition. Science. 1997; 277:1094–1097. [PubMed: 9262477]

NIH-PA Author Manuscript NIH-PA Author Manuscript NIH-PA Author Manuscript

2. Cravatt BF, Giang DK, Mayfield SP, Boger DL, Lerner RA, Gilula NB. Molecular characterization of an enzyme that degrades neuromodulatory fatty-acid amides. Nature. 1996; 384:83–87. [PubMed: 8900284]
3. Degenhardt BF, Darmani NA, Johnson JC, Towns LC, Rhodes DC, Trinh C, McClanahan B, DiMarzo V. Role of osteopathic manipulative treatment in altering pain biomarkers: a pilot study. Am. Osteopath. Assoc. 2007; 107:387–400.
4. Matsuda LA, Lolait SJ, Brownstein MJ, Young AC, Bonner TI. Structure of a cannabinoid receptor and functional expression of the cloned cDNA. Nature. 1990; 346:561–564. [PubMed: 2165569]
5. Munro S, Thomas KL, Abu-Shaar M. Molecular characterization of aperipheral receptor for cannabinoids. Nature. 1993; 365:61–65. [PubMed: 7689702]
6. Sanchez C, de Ceballos ML, Gomez del Pulgar T, Rueda D, Corbacho C, Velasco G, Galve-Roperh I, Huffman JW, Ramon y, Cajal S, Guzman M. Inhibition of glioma growth in vivo by selective activation of the CB(2) cannabinoid receptor. Cancer Res. 2001; 61:5784–5789. [PubMed: 11479216]
7. Fernandez-Ruiz J, Romero J, Velasco G, Tolon RM, Ramos JA, Guzman M. Cannabinoid CB2 receptor: a new target for controlling neural cell survival? Trends Pharmacol. Sci. 2007; 28:39–45. [PubMed: 17141334]
8. Svizenska I, Dubovy P, Sulcova A. Cannabinoid receptors 1 and 2 (CB1 and CB2), their distribution, ligands and functional involvement involvement in nervous system structures—a short review. Pharmacol., Biochem. Behav. 2008; 90:501–511. [PubMed: 18584858]
9. Hohmann AG. Spinal and peripheral mechanisms of cannabinoid antinociception: behavioral, neurophysiological and neuroanatomical perspectives. Chem. Phys. Lipids. 2002; 121:173–190. [PubMed: 12505699]
10. Karsak M, Gaffal E, Date R, Wang-Eckhardt L, Rehnelt J, Petrosino S, Starowicz K, Steuder R, Schlicker E, Cravatt B, Mechoulam R, Buettner R, Werner S, Di Marzo V, Tuting T, Zimmer A. Attenuation of allergic contact dermatitis through the endocannabinoid system. Science. 2007; 316:1494–1497. [PubMed: 17556587]
11. Palazuelos J, Davoust N, Julien B, Hatterer E, Aguado T, Mechoulam R, Benito C, Romero J, Silva A, Guzman M, Nataf S, Galve-Roperh I. The CB2 cannabinoid receptor controls myeloid progenitor trafficking. J. Biol. Chem. 2008; 283:13320–13329. [PubMed: 18334483]
12. Guindon J, Hohmann AG. The endocannabinoid system and cancer: therapeutic implication. Br. J. Pharmacol. 2011; 163:1447–1463. [PubMed: 21410463]
13. Oesch S, Gertsch J. Cannabinoid receptor ligands as potential anticancer agents—high hopes for new therapies? J. Pharm. Pharmacol. 2009; 61:839–853. [PubMed: 19589225]
14. Idris AI, Ralston SH. Cannabinoids and bone: friend or foe? Calcif. Tissue Int. 2010; 87:285–297. [PubMed: 20532878]
15. Izzo AA, Camilleri M. Emerging role of cannabinoids in gastrointestinal and liver diseases: basic and clinical aspects. Gut. 2008; 57:1140–1155. [PubMed: 18397936]
16. Munoz-Luque J, Ros J, Fernandez-Varo G, Tugues S, Morales-Ruiz M, Alvarez CE, Friedman SL, Arroyo V, Jimenez W. Regression of fibrosis after chronic stimulation of cannabinoid CB2 receptor in cirrhotic rats. J. Pharmacol. Exp. Ther. 2008; 324:475–483. [PubMed: 18029545]
17. Pacher P, Batkai S, Kunos G. The endocannabinoid system as an emerging target of pharmacotherapy. Pharmacol. Rev. 2006; 58:389–462. [PubMed: 16968947]
18. Compton DR, Rice KC, De Costa BR, Razdan RK, Melvin LS, Johnson MR, Martin B. R Cannabinoid structure- activity relationships: correlation of receptor binding and in vivo activities. J. Pharmacol. Exp. Ther. 1993; 265:218–226. [PubMed: 8474008]
19. Huffman JW. Cannabimimetic indoles, pyrroles and indenes. Curr. Med. Chem. 1999; 6:705–720. [PubMed: 10469887]
20. Palmer SL, Thakur GA, Makriyannis A. Cannabinergic ligands. Chem. Phys. Lipids. 2002; 121:3–19. [PubMed: 12505686]
21. Raitio KH, Salo OM, Nevalainen T, Poso A, Jarvinen T. Targeting the cannabinoid CB2 receptor: mutations, modeling and development of CB2 selective ligands. Curr. Med. Chem. 2005; 12:1217–1237. [PubMed: 15892633]

NIH-PA Author Manuscript NIH-PA Author Manuscript NIH-PA Author Manuscript

22. Marriott KS, Huffman JW. Recent advances in the development of selective ligands for the cannabinoid CB(2) receptor. Curr. Top. Med. Chem. 2008; 8:187–204. [PubMed: 18289088]
23. Yang P, Wang L, Xie XQ. Latest advances in novel cannabinoid CB(2) ligands for drug abuse and their therapeutic potential. Future Med. Chem. 2012; 4:187–204. [PubMed: 22300098]
24. Rinaldi-Carmona M, Barth F, Millan J, Derocq JM, Casellas P, Congy C, Oustric D, Sarran M, Bouaboula M, Calandra B, Portier M, Shire D, Breliere JC, Le Fur GL. SR 144528, the first potent and selective antagonist of the CB2 cannabinoid receptor. J. Pharmacol. Exp. Ther. 1998; 284:644–650. [PubMed: 9454810]
25. Ross RA, Brockie HC, Stevenson LA, Murphy VL, Templeton F, Makriyannis A, Pertwee RG. Agonist-inverse agonist characterization at CB1 and CB2 cannabinoid receptors of L759633, L759656, and AM630. Br. J. Pharmacol. 1999; 126:665–672. [PubMed: 10188977]
26. Iwamura H, Suzuki H, Ueda Y, Kaya T, Inaba T. In vitro and in vivo pharmacological characterization of JTE-907, a novel selective ligand for cannabinoid CB2 receptor. J. Pharmacol. Exp. Ther. 2001; 296:420–425. [PubMed: 11160626]
27. Lunn CA, Fine JS, Rojas-Triana A, Jackson JV, Fan X, Kung TT, Gonsiorek W, Schwarz MA, Lavey B, Kozlowski JA, Narula SK, Lundell DJ, Hipkin RW, Bober LA. A novel cannabinoid peripheral cannabinoid receptor-selective inverse agonist blocks leukocyte recruitment in vivo. J. Pharmacol. Exp. Ther. 2006; 316:780–788. [PubMed: 16258021]
28. Schuehly W, Paredes JM, Kleyer J, Huefner A, Anavi-Goffer S, Raduner S, Altmann KH, Gertsch J. Mechanisms of osteoclastogenesis inhibition by a novel class of biphenyl-type cannabinoid CB(2) receptor inverse agonists. Chem. Biol. 2011; 18:1053–1064. [PubMed: 21867920]
29. Giblin GM, O'Shaughnessy CT, Naylor A, Mitchell WL, Eatherton AJ, Slingsby BP, Rawlings DA, Goldsmith P, Brown AJ, Haslam CP, Clayton NM, Wilson AW, Chessell IP, Wittington AR, Green R. Discovery of 2-[(2,4-dichlorophenyl)-amino]-N-[(tetrahydro-2H-pyran-4-yl)methyl]-4-(trifluoromethyl)-5-pyrimidinecarboxamide, a selective CB2 receptor agonist for the treatment of inflammatory pain. J. Med. Chem. 2007; 50:2597–2600. [PubMed: 17477516]
30. Xi Z-X, Peng X-Q, Li X, Song R, Zhang H-Y, Liu Q-R, Yang H-J, Bi G-H, Li J, Gardner EL. Brain cannabinoid CB2 receptors modulate cocaine's actions in mice. Nat. Neurosci. 2011; 14:1160–1166. [PubMed: 21785434]
31. Gertsch J, Leonti M, Raduner S, Racz I, Chen JZ, Xie XQ, Altmann KH, Karsak M, Zimmer A. Beta-caryophyllene is a dietary cannabinoid. Proc. Natl. Acad. Sci. U.S.A. 2008; 105:9099–9104. [PubMed: 18574142]
32. Zhong H, Bowen JP. GALAHAD pharmacophore modeling for drug discovery. J. Am. Chem. Soc. 2007; 129:5780–5780.
33. SYBYL 8.0. St. Louis, MO, U.S: Tripos; 2007.
34. Xie XQ, Chen J. Data-mining a small molecule drug screening representative subset from NIH PubChem database. J. Chem. Inf. Model. 2008; 48:465–475. [PubMed: 18302356]
35. Francisco ME, Seltzman HH, Gilliam AF, Mitchell RA, Rider SL, Pertwee RG, Stevenson LA, Thomas BF. Synthesis and structure-activity relationships of amide and hydrazide analogues of the cannabinoid CB(1) receptor antagonist N-(piperidinyl)-5-(4-chlorophenyl)-1-(2,4-dichlorophenyl)-4-methyl-1H-pyrazole-3-carbox-amide (SR141716). J. Med. Chem. 2002; 45:2708–2719. [PubMed: 12061874]
36. Zhang Y, Xie Z, Wang L, Schreiter B, Lazo JS, Gertsch J, Xie XQ. Mutagenesis and computer modeling studies of a GPCR conserved residue W5.43(194) in ligand recognition and signal transduction for CB2 receptor. Int. Immunopharmacol. 2011; 11:1303–1310. [PubMed: 21539938]
37. Anandarajah AP, Schwarz EM, Totterman S, Monu J, Feng CY, Shao T, Haas-Smith SA, Ritchlin CT. The effect of etanercept on osteoclast precursor frequency and enhancing bone marrow oedema in patients with psoriatic arthritis. Ann. Rheum. Dis. 2008; 67:296–301. [PubMed: 17967829]
38. Myint KZ, Xie X-Q. Recent advances in fragment-based QSAR and multi-dimensional QSAR methods. Int. J. Mol. Sci. 2010; 11:3846–3866. [PubMed: 21152304]
39. Chen J-Z, Han X-W, Liu Q, Makriyannis A, Wang J, Xie X-Q. 3D-QSAR studies of arylpyrazole antagonists of cannabinoid receptor subtypes CB1 and CB2. A combined NMR and CoMFA approach. J. Med. Chem. 2006; 49:625–636. [PubMed: 16420048]

NIH-PA Author Manuscript

NIH-PA Author Manuscript

NIH-PA Author Manuscript

40. Xie XQ, Melvin LS, Makriyannis A. The conformational properties of the highly selective cannabinoid receptor ligand CP-55,940. J. Biol. Chem. 1996; 271:10640–10647. [PubMed: 8631869]
41. Xie X-Q, Chen J-Z, Billings EM. 3D structural model of the G-protein-coupled cannabinoid CB2 receptor. Proteins: Struct., Funct., Bioinf. 2003; 53:307–319.
42. Diaz P, Phatak SS, Xu J, Astruc-Diaz F, Cavasotto CN, Naguib M. 6-Methoxy-N-alkyl isatin acylhydrazone derivatives as a novel series of potent selective cannabinoid receptor 2 inverse agonists: design, synthesis, and binding mode prediction. J. Med. Chem. 2008; 52:433–444. [PubMed: 19115816]
43. Gouldson P, Calandra B, Legoux P, Kerneis A, Rinaldi-Carmona M, Barth F, Le Fur G, Ferrara P, Shire D. Mutational analysis and molecular modeling of the antagonist SR 144528 binding site on the human cannabinoid CB2 receptor. Eur. J. Pharmacol. 2000; 401:17–25. [PubMed: 10915832]
44. Poso A, Huffman JW. Targeting the cannabinoid CB2 receptor: modelling and structural determinants of CB2 selective ligands. Br. J. Pharmacol. 2008; 153:335–346. [PubMed: 17982473]
45. Wan JP, Chai YF, Wu JM, Pan YJ. *N*,*N*′-(Phenylmethylene)diacetamide analogues as economical and efficient ligands in copper-catalyzed arylation of aromatic nitrogen-containing heterocycles. Synlett. 2008:3068–3072.
46. Bayer A, Maier ME. Synthesis of enamides from aldehydes and amides. Tetrahedron. 2004; 60:6665–6677.
47. Feng R, Anderson G, Xiao G, Elliott G, Leoni L, Mapara MY, Roodman GD, Lentzsch S. SDX-308, a nonsteroidal anti-inflammatory agent, inhibits NF-kappaB activity, resulting in strong inhibition of osteoclast formation/activity and multiple myeloma cell growth. Blood. 2007; 109:2130–2138. [PubMed: 17095620]
48. Feng R, Ma H, Hassig CA, Payne JE, Smith ND, Mapara MY, Hager JH, Lentzsch S. KD5170, a novel mercaptoketone-based histone deacetylase inhibitor, exerts antimyeloma effects by DNA damage and mitochondrial signaling. Mol. Cancer Ther. 2008; 7:1494–1505. [PubMed: 18566220]
49. SYBYL X1.2. 1699 South Hanley Rd, St. Louis, MO, 63144, U.S.: Tripos; software available at www.tripos.com

NIH-PA Author Manuscript

NIH-PA Author Manuscript

NIH-PA Author Manuscript

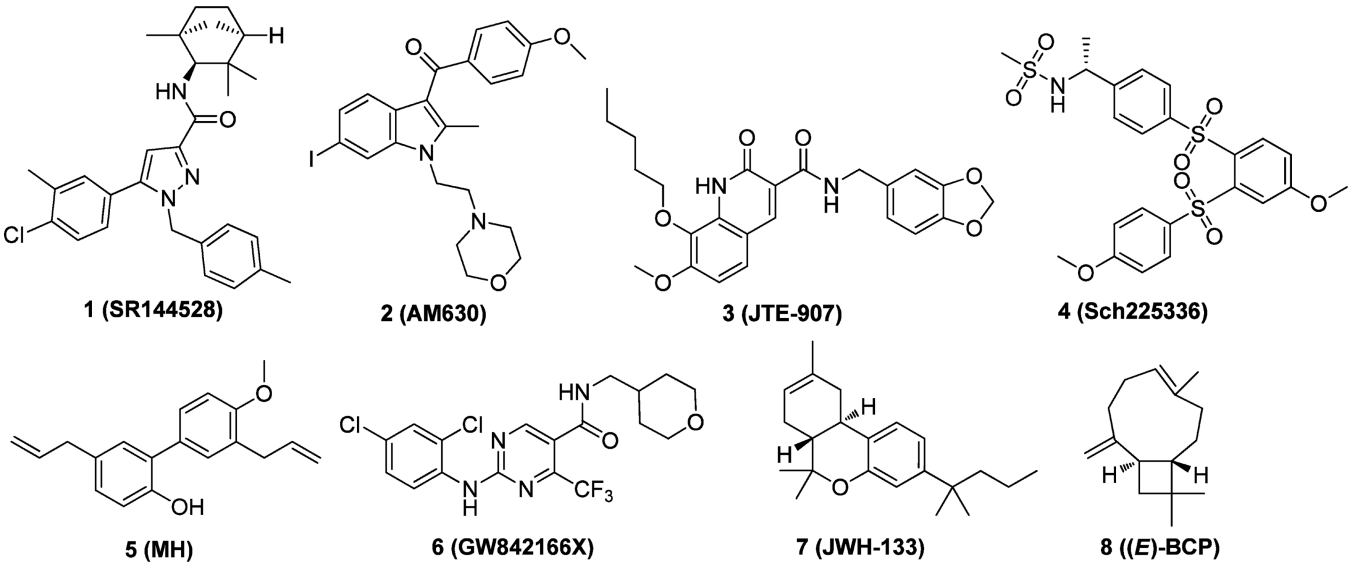

Figure 1.
Representative CB_2 receptor-selective compounds with various chemical scaffolds.

NIH-PA Author Manuscript

NIH-PA Author Manuscript

NIH-PA Author Manuscript

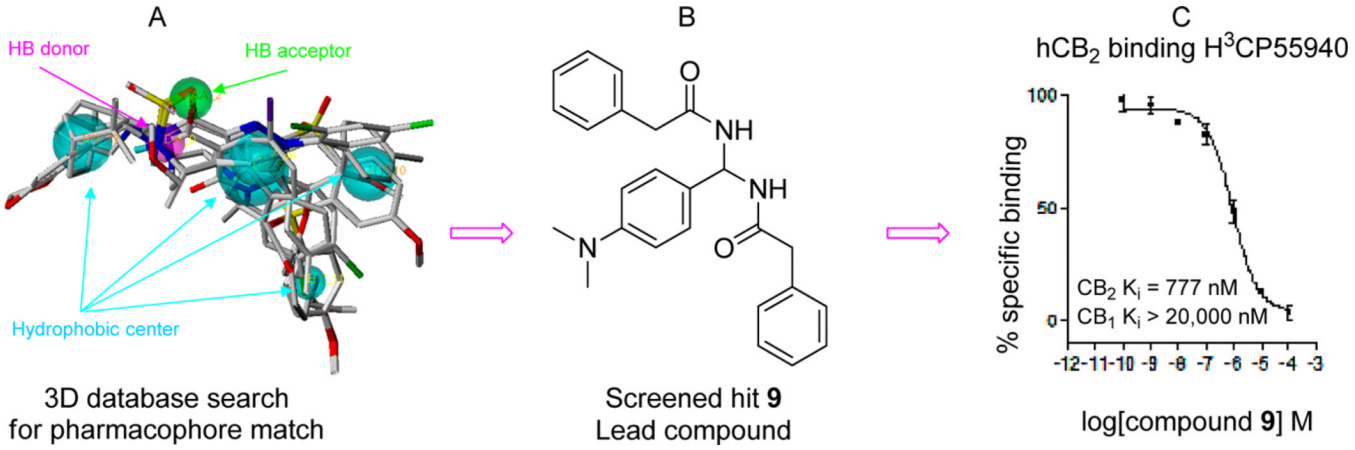

Figure 2.

Novel CB_2 ligand **9** discovered by 3D pharmacophore database virtual screening search and confirmed by experimental bioassays: (A) pharmacophore query; (B) virtually screened hit **9**; (C) **9** validated by [^{3}H]CP-55040 radiometric binding assays showing high CB_2 receptor binding affinity, K_i = 777 nM and selectivity (>26-fold).

NIH-PA Author Manuscript

NIH-PA Author Manuscript

NIH-PA Author Manuscript

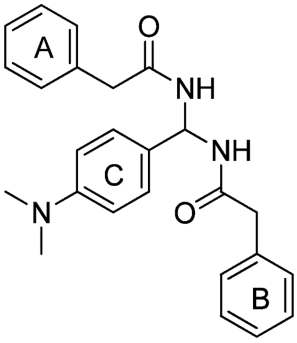

Compound **9**:
CB_2 K_i = 777 nM
CB_1 K_i > 20,000 nM
Selectivity CB_1/CB_2 > 26

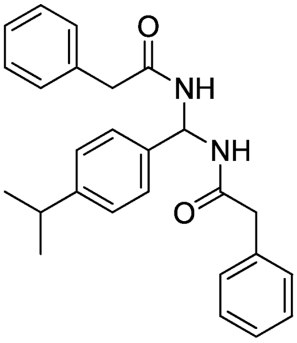

Compound **18**:
EC_{50} = 4 nM, CB_2 K_i = 85 nM
CB_1 K_i > 20,000 nM
Selectivity CB_1/CB_2 > 235

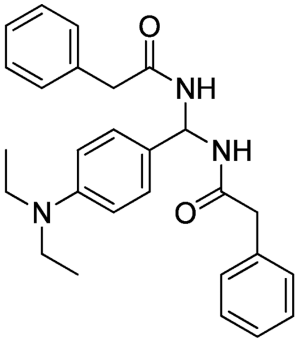

Compound **26**:
EC_{50} = 5 nM, CB_2 K_i = 64 nM
CB_1 K_i > 20,000 nM
Selectivity CB_1/CB_2 > 313

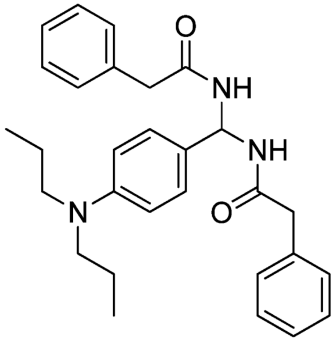

Compound **27**:
EC_{50} = 28 nM, CB_2 K_i = 22 nM
CB_1 K_i > 20,000 nM
Selectivity CB_1/CB_2 > 909

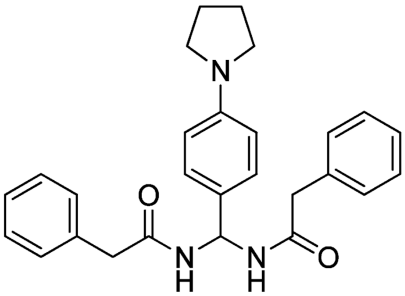

Compound **30**:
EC_{50} = 17 nM, CB_2 K_i = 71 nM
CB_1 K_i > 20,000 nM
Selectivity CB_1/CB_2 > 281

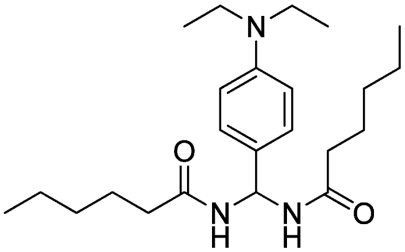

Compound **59**:
EC_{50} = 13 nM, CB_2 K_i = 25 nM
CB_1 K_i > 20,000 nM
Selectivity CB_1/CB_2 > 800

Figure 3.
Structures of the lead compound **9** and the modified target compounds **18, 26, 27, 30**, and **59**.

NIH-PA Author Manuscript

NIH-PA Author Manuscript

NIH-PA Author Manuscript

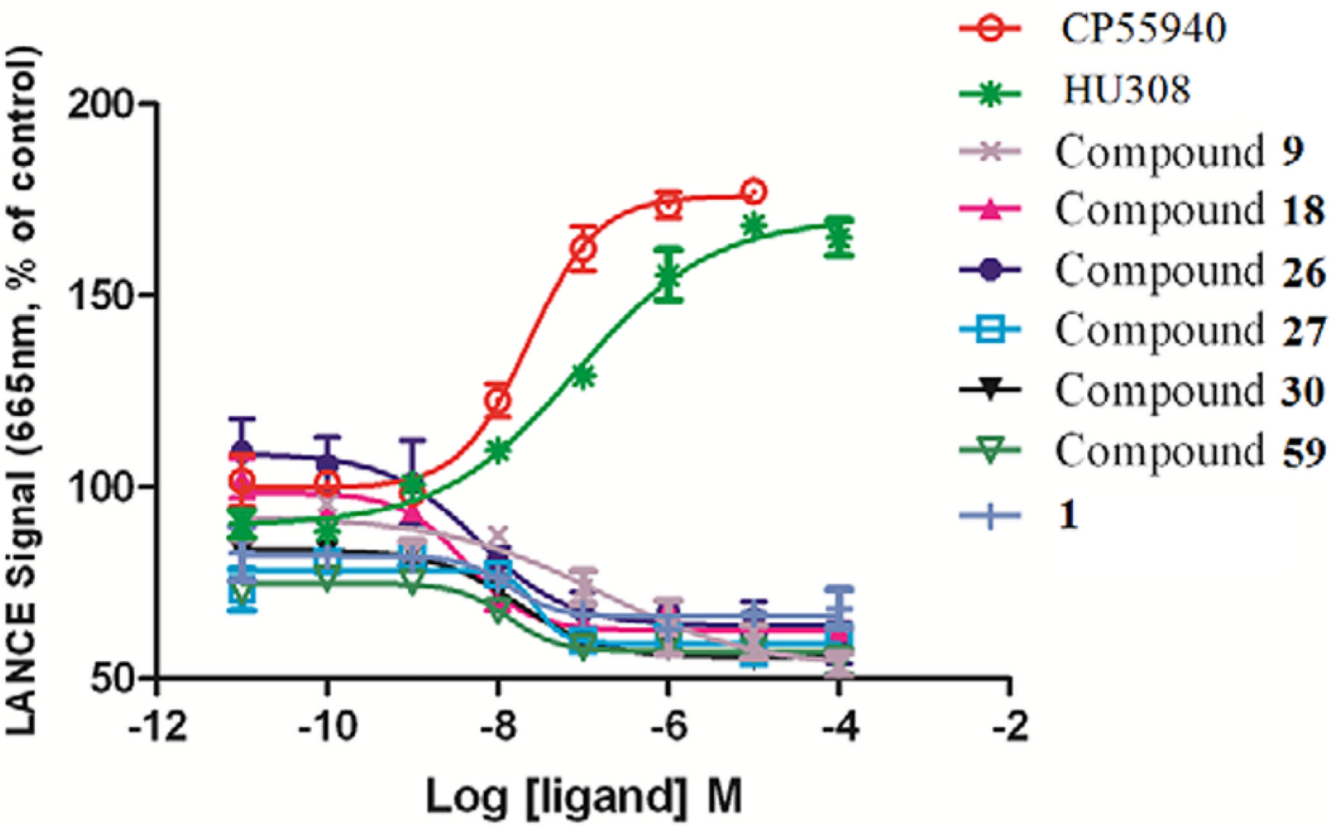

Figure 4.

Comparisons of LANCE signal of different CB_2 receptor ligands in stably transfected CHO cells expressing human CB_2 receptors in a concentration-dependent fashion. EC_{50} values of compounds **9, 18, 26, 27, 30, 59**, and **1** are 159.1 ± 8.68, 4.11 ± 3.66, 5.73 ± 6.37, 28.33 ± 2.54,17.08 ± 2.11, 13.42 ± 2.07, and 13.7 ± 2.81 nM, respectively EC_{50} for CP-55,940 and HU308 are 23.29 ± 4.17 and 83.81 ± 5.63 nM. Data are the mean ± SEM of one representative experiment of two or more performed in duplicate or triplicate.

NIH-PA Author Manuscript

NIH-PA Author Manuscript

NIH-PA Author Manuscript

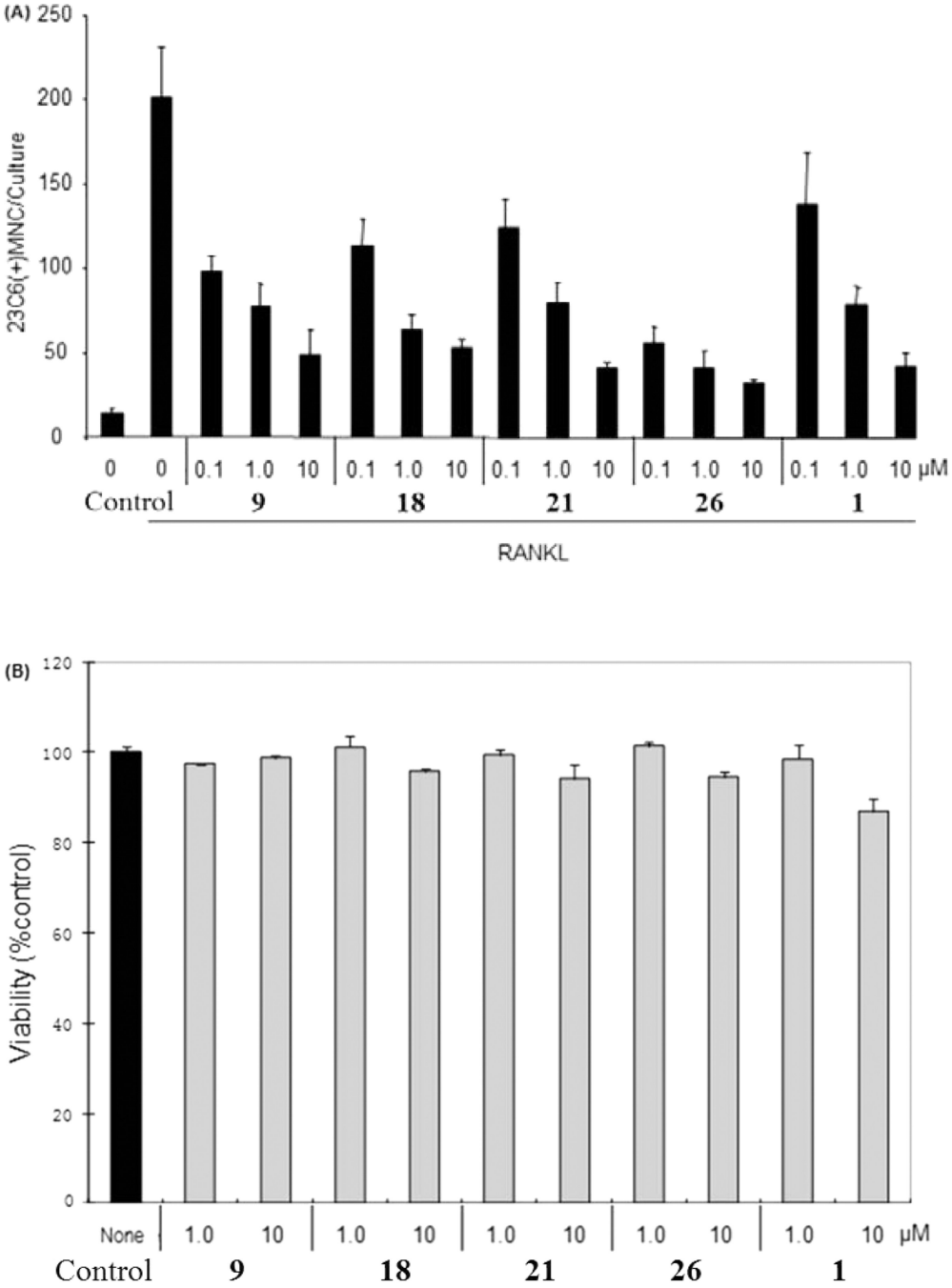

Figure 5.

Inhibition of human osteoclastogenesis by CB_2 ligands. (A) Human-bone-marrow-derived mononuclear cells were cultured in a 96-well plate for 3 weeks in the presence of RANKL (50 ng/mL) to form osteoclast-like cells, as described in the Experimental Section. After 3 weeks, the cultures were stained with the 23c6 antibody. 23c6-positive OCLs containing three or more nuclei were scored microscopically. All experiments were performed in triplicate. Results are shown as the mean ± SD. SR = SR144528. The control on the left is vehicle control, and the right one is positive control. (B) Cytotoxic effects of PAM compounds on normal human mononuclear cells. Samples of primary PBMCs (10^5 cells per well in 96-well plate) from healthy donors were treated in culture for 72 h with the indicated

compounds. The viability of cells was determined using trypan blue exclusion assay. The results were presented as the mean ± SD of three assays.

NIH-PA Author Manuscript

NIH-PA Author Manuscript

NIH-PA Author Manuscript

NIH-PA Author Manuscript

NIH-PA Author Manuscript

NIH-PA Author Manuscript

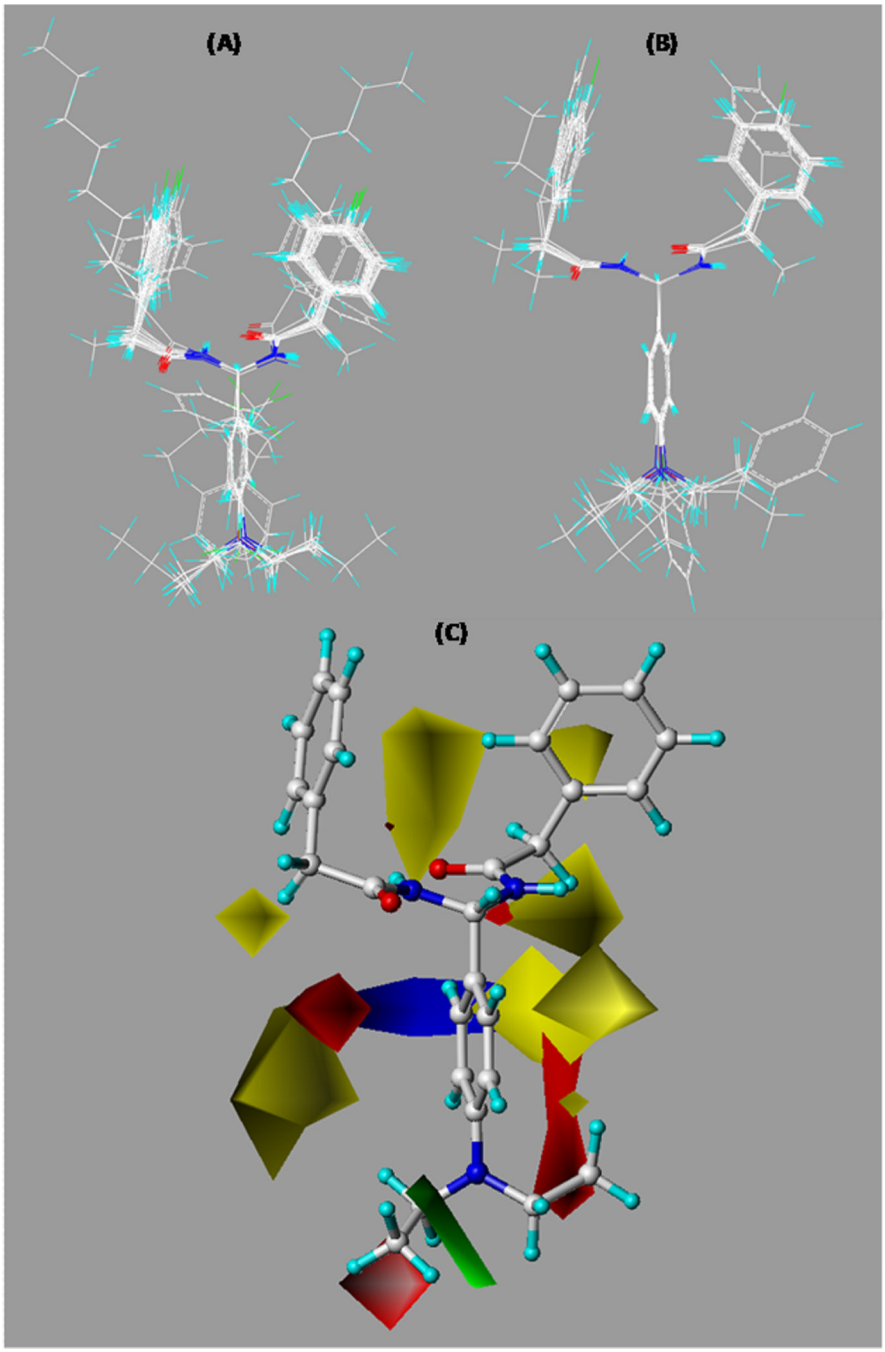

Figure 6.

Overall alignments of training set molecules (A) and test set molecules (B) to compound **26** and CoMFA contour maps of compound **26** showing steric and electrostatic (C) interactions. Sterically (bulk) favored areas are color-coded in green, and sterically unfavored areas are in yellow. Electrostatically (charge) preferred regions are in blue, and red regions are electrostatically unfavored areas.

NIH-PA Author Manuscript

NIH-PA Author Manuscript

NIH-PA Author Manuscript

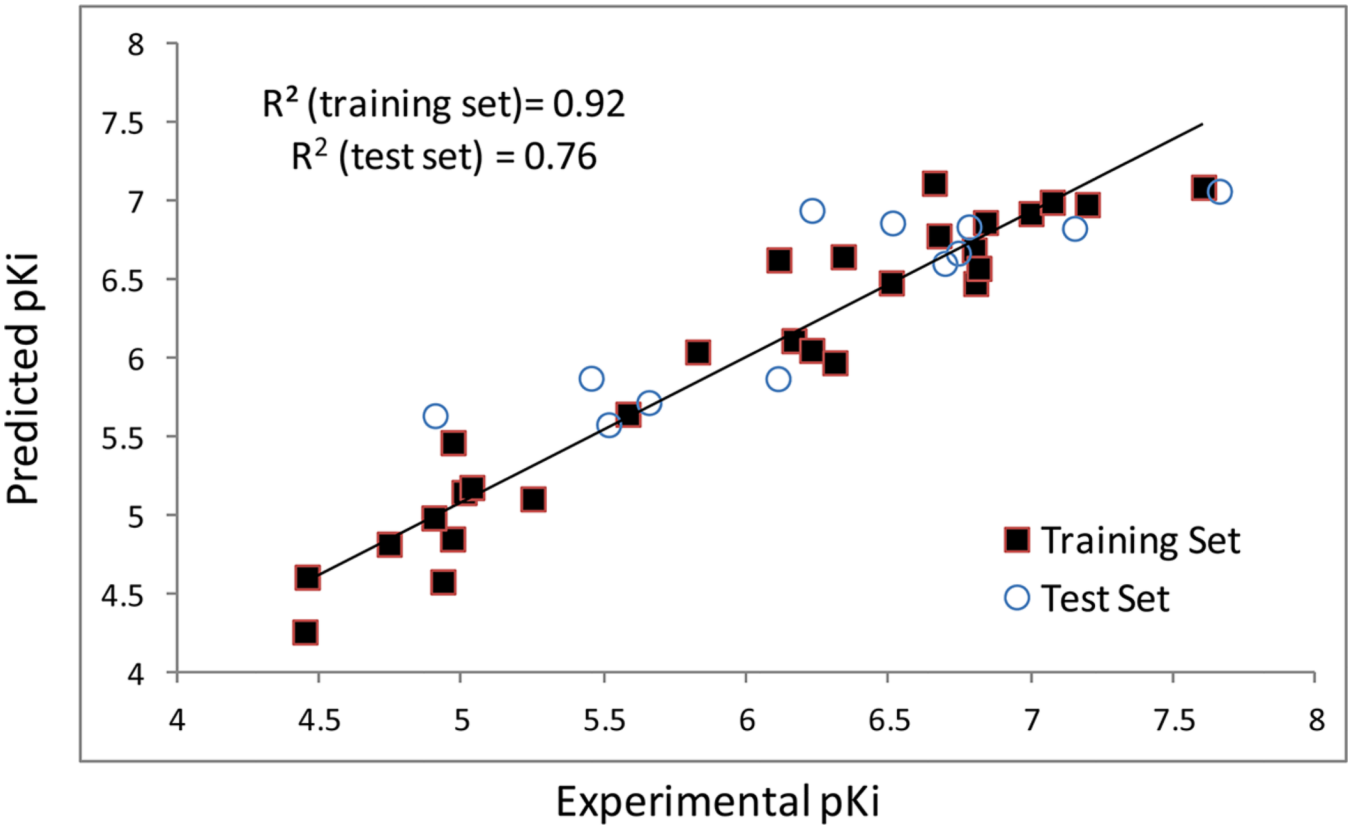

Figure 7.
Plots of CoMFA-calculated and experimental binding affinity values (pK_i) for the training and test sets.

NIH-PA Author Manuscript

NIH-PA Author Manuscript

NIH-PA Author Manuscript

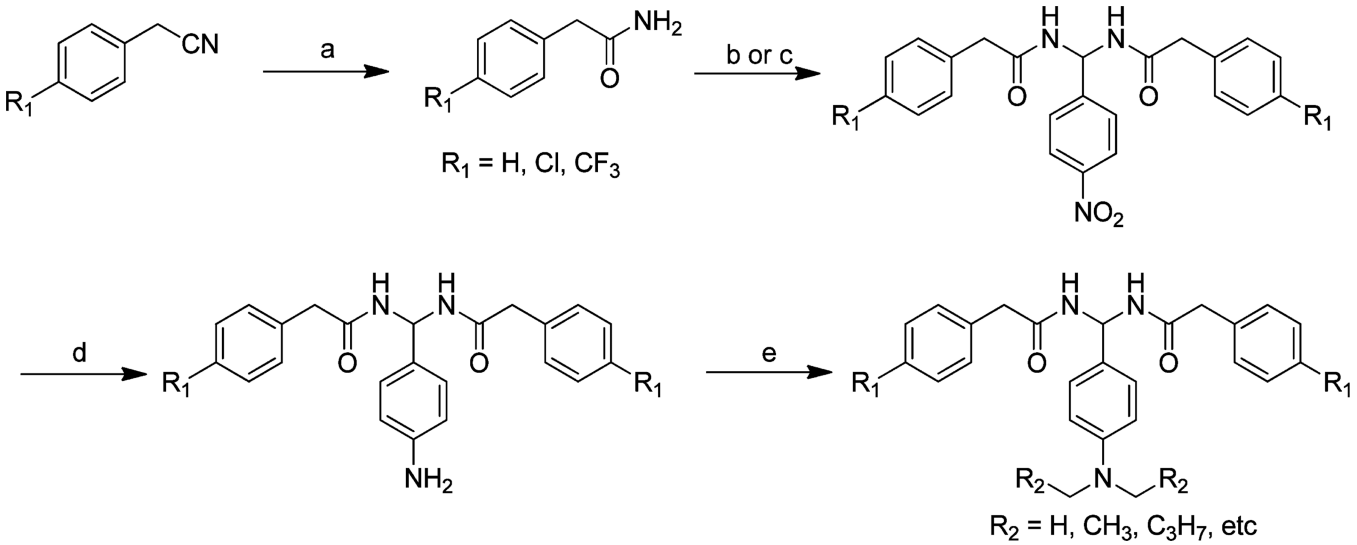

Scheme 1.

General Synthesis of PAM Derivativesa

[a]Reagents and conditions: (a) concentrated H_2SO_4, 0 °C, 12 h. (b) Method 1: aldehyde, anhydrous dichloroethane, TMSCl, 70 °C, 3–12 h. (c) Method 2: aldehyde, anhydrous dichloromethane, $F_3CSO_3SiMe_3$, rt, 12 h. (d) Ethanol, palladium (10%), hydrazine, 70 °C, 3 h. (e) DMF, K_2CO_3, rt, 12 h.

NIH-PA Author Manuscript
NIH-PA Author Manuscript
NIH-PA Author Manuscript

Table 1

Radioligand Competition Binding Affinity(K_i)Data of PAM Derivatives

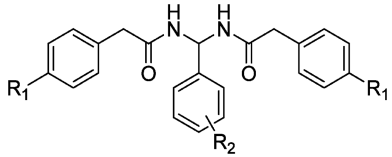

compd	R_1	R_2	MW	cLogP	K_i (CB_2), nM[a,b]	K_i (CB_1, nM[a,c]	SI[d]
9	H	*p*-$(CH_3)_2N$-	401.50	4.04	777	>20000	>26
11	H	H-	358.43	3.93	9930	NT	
12	H	*o*-F-	376.42	4.08	35330	NT	
13	H	*m*-F-	376.42	4.08	12670	NT	
14	H	*p*-F-	376.42	4.08	10900	NT	
15	H	*p*-Cl-	392.88	4.54	3081	NT	
16	H	*p*-Br-	437.33	4.70	2226	NT	
17	H	*p*-CH_3-	372.46	4.45	494	109	
18	H	*p*-*i*-C_3H_7-	400.51	5.18	85	>20000	>235
19	H	*p*-CH_3O-	388.46	3.78	783	>20000	>26
20	H	*p*-C_2H_sO-	402.49	4.13	1500	NT	
21	H	*p*-*i*-C_3H_7O-	416.51	4.55	313	>20000	>64
22	H	*o*-CF_3-	426.43	4.81	11780	NT	
23	H	*p*-CF_3-	426.43	4.81	596	>20000	>34
24	H	*p*-NO_2	403.43	3.87	NB	NT	
25	H	*p*-H_2N-	373.45	2.51	12550	NT	
26	H	*p*-$(C_2H_5)_2N$-	429.55	4.76	64	>20000	>313
27	H	*p*-$(C_3H_7)_2N$-	457.61	5.80	22	>20000	>909
28	H	*p*-$(C_4H_9)_2N$-	485.66	6.69	221	>20000	>90
29	H	*p*-$(benzyl)_2N$-	553.69	7.33	203	>20000	>99
30	H	*p*-pyrrolidinyl-	427.53	4.45	71	>20000	>281
31	H	*p*-piperidyl-	441.56	4.89	595	>20000	>34

NIH-PA Author Manuscript
NIH-PA Author Manuscript
NIH-PA Author Manuscript

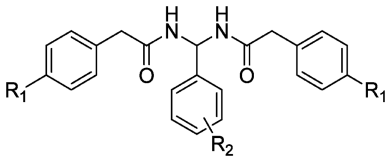

compd	R_1	R_2	MW	cLogP	K_i (CB_2), nM[a,b]	K_i (CB_1, nM[a,c]	SI[d]
32	Cl	H-	427.32	5.14	NB	NT	
33	Cl	*o*-F-	445.31	5.29	10850	NT	
34	Cl	*p*-F-	445.31	5.29	NB	NT	
35	Cl	*p*-Cl-	461.77	5.75	154	>20000	>130
36	Cl	*p*-CH_3-	441.35	5.66	462	>20000	>43
37	Cl	*p*-CH_3O-	457.35	4.98	310	>20000	>65
38	Cl	*o*-CF_3-	495.32	6.02	158	>20000	>127
39	Cl	*p*-CF_3-	495.32	6.02	101	>20000	>198
40	Cl	*p*-NO_2-	472.32	5.08	NB	NT	
41	CF_3	H-	494.43	5.69	NB	NT	
42	CF_3	*o*-F-	512.42	5.83	NB	NT	
43	CF_3	*p*-F-	512.42	5.83	NB	NT	
44	CF_3	*p*-Cl-	528.87	6.29	NB	NT	
45	CF_3	*p*-CH_3-	508.46	6.20	NB	NT	
46	CF_3	*p*-CH_3O-	524.45	5.53	NB	NT	
47	CF_3	*p*-CF_3-	562.43	6.57	NB	NT	
1[e,f]					2.1	NT	
10[e,g]					NT	10.6	

[a]Binding affinities of compounds for CB_1 and CB_2 receptor were evaluated using [^{3}H]CP-55,940 radioligand competition binding assay.

[b]NB: no binding, K_i > 20000 nM.

[C]NT: not tested.

[d]SI: selectivity index for CB_2, calculated as $K_i(CB_1)/K_i(CB_2)$ ratio.

[e]The binding affinities of reference compounds were evaluated in parallel with compounds **9, 11–61** under the same conditions.

[f] CB_2 reference compound SR144528.

[g] CB_1 reference compound SR141716.

NIH-PA Author Manuscript

NIH-PA Author Manuscript

NIH-PA Author Manuscript

NIH-PA Author Manuscript
NIH-PA Author Manuscript
NIH-PA Author Manuscript

Table 2

Radioligand Competition Binding Affinity(K_i) Data of PAM Derivatives

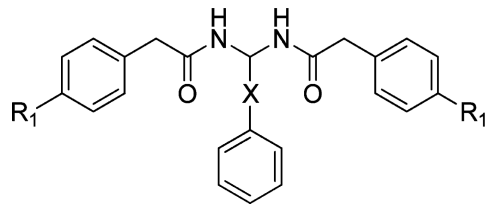

compd	R_i	X	MW	cLogP	K_i(CB$_2$), nM[a,b,c]	K_i(CB$_1$), nM[a,b,c]
48	H	CH_2	372.46	3.99	NB	NB
49	H	CH_2CH_2	386.49	4.44	9,319	NB
50	H	CH=CH	384.47	4.54	5,683	NB
1[d,e]					2.1	NT
10[d,f]					NT	10.6

[a]Binding affinities of compounds for CB$_1$ and CB$_2$ receptor were evaluated using [^{3}H]CP-55,940 radioligand competition binding assay.

[b]NB: no binding, K_i > 20000 nM.

[C]NT: not tested.

[d]The binding affinities of reference compounds were evaluated in parallel with compounds **9, 11–61** under the same conditions.

[e]CB$_2$ reference compound SR144528.

[f]CB$_1$ reference compound SR141716.

NIH-PA Author Manuscript
NIH-PA Author Manuscript
NIH-PA Author Manuscript

Table 3

Radioligand Competition Binding Affinity (K_i) Data of PAM Derivatives

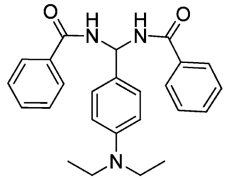

Compound **51**

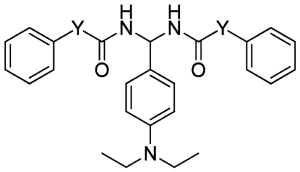

compd	Y	MW	cLogP	K_i (CB$_2$), nM[a,b]	K_i (CB$_1$), nM[a,c]	SI[d]
51		401.50	4.80	688	>20000	>29
52	CH_2CH_2	457.61	5.64	213	>20000	>93
53	CH=CH	453.58	5.80	167	>20000	>119
1[e,f]				2.1	NT	
10[e,g]				NT	10.6	

[a] Binding affinities of compounds for CB$_1$ and CB$_2$ receptor were evaluated using [^{3}H]CP-55,940 radioligand competition binding assay.

[b] NB: no binding, K_i > 20000 nM.

[c] NT: not tested.

[d] SI: selectivity index for CB$_2$, calculated as K_i(CB$_1$)/K_i(CB$_2$) ratio.

[e] The binding affinities of reference compounds were evaluated in parallel with compounds **9, 11–61** under the same conditions.

[f] CB$_2$ reference compound SR144528.

[g] CB$_1$ reference compound SR141716.

NIH-PA Author Manuscript
NIH-PA Author Manuscript
NIH-PA Author Manuscript

Table 4

Radioligand Competition Binding Affinity (K_i) Data of PAM Derivatives

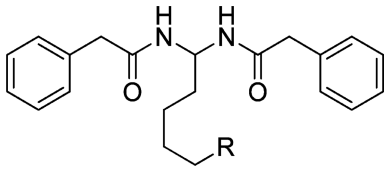

compd	R	MW	cLogP	K_i (CB_2), nM[a,b]	K_i (CB_1, nM[a,c]
54	H	338.44	3.75	35970	NT
55	CH_3	352.47	4.19	18200	NB
1[d,e]				2.1	NT
10[d,f]				NT	10.6

[a]Binding affinities of compounds for CB_1 and CB_2 receptor were evaluated using [^{3}H]CP-55,940 radioligand competition binding assay

[b]NB: no binding, K_i > 20000 nM.

[c]NT: not tested.

[d]The binding affinities of reference compounds were evaluated in parallel with compounds **9, 11–61** under the same conditions.

[e]CB_2 reference compound SR144528.

[f]CB_1 reference compound SR141716.

NIH-PA Author Manuscript
NIH-PA Author Manuscript
NIH-PA Author Manuscript

Table 5

Radioligand Competition Binding Affinity(K_i)Data of PAM Derivatives

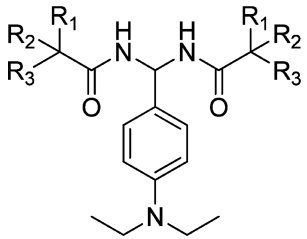

Compd	R_i	R_2	R_3	MW	cLog P	K_i (CB_2), nM[a,b]	K_i (CB_1), nM[a,c]	SI[d]
56	H	CH_3	CH_3	333.46	3.57	2636	NB	
57	CH_3	CH_3	CH_3	361.52	4.69	3553	NB	
58	H	H	C_3H_7	361.52	4.27	182	>20000	>109
59	H	H	C_4H_9	389.57	5.16	25	>20000	>800
60	H	H	C_6H_{13}	445.68	7.9	146	>20000	>136
61	H	H	C_8H_{17}	501.79	10.0	160	>20000	>125
1[e,f]						2.1	NT	
1[e,g]						NT	10.6	

[a]Binding affinities of compounds for CB_1 and CB_2 receptor were evaluated using [^{3}H]CP-55,940 radioligand competition binding assay.

[b]NB: no binding, K_i > 20000 nM.

[c]NT: not tested.

[d]SI: selectivity index for CB_2, calculated as $K_i(CB_1)/K_i(CB_2)$ ratio.

[e]The binding affinities of reference compounds were evaluated in parallel with compounds **9, 11–61** under the same conditions.

[f]CB_2 reference compound SR144528.

[g]CB_1 reference compound SR141716.

NIH-PA Author Manuscript

NIH-PA Author Manuscript

NIH-PA Author Manuscript

Table 6

Experimental (expt) and Predicted (pred) pK_i Values of PAM Derivatives in the Training Set and Test Set

Compd	pK_i (expt)	P-K_j (pred)	residual
9	6.109579	6.63026	−0.5207
11	5.003051	5.15014	−0.1471
12	4.451856	4.61118	−0.1593
13	4.897223	4.98821	−0.091
14	4.962574	4.85432	0.10825
15[a]	5.511308	5.58159	−0.0703
16[a]	5.652475	5.72248	−0.07
17	6.306273	5.97563	0.33064
18	7.070581	6.99702	0.07356
19[a]	6.106238	5.87445	0.23179
20	5.823909	6.04419	−0.2203
21	6.504456	6.48389	0.02057
22	4.928855	4.58176	0.3471
23	6.224754	6.05444	0.17031
25[a]	4.901356	5.63905	−0.7377
26	7.19382	6.98267	0.21115
27[a]	7.657577	7.06706	0.59052
28	6.655608	7.11863	−0.463
29[a]	6.692504	6.60822	0.08428
30[a]	7.148742	6.83115	0.31759
31[a]	6.225483	6.94563	−0.7201
33	4.96457	5.46751	−0.5029
35	6.812479	6.5766	0.23588
36	6.335358	6.6504	−0.315
37[a]	6.508638	6.86546	−0.3568
38	6.801343	6.47965	0.32169
39	6.995679	6.92502	0.07066
49	5.030631	5.18212	−0.1515
50	5.245422	5.10916	0.13626
51	6.162412	6.11595	0.04646
52	6.67162	6.78351	−0.1119
53[a]	6.777284	6.84095	−0.0637
54	4.44406	4.26222	0.18184
55	4.739929	4.82097	−0.081
56	5.579055	5.64843	−0.0694
57[a]	5.449405	5.87713	−0.4277
58[a]	6.739929	6.67326	0.06667

NIH-PA Author Manuscript

NIH-PA Author Manuscript

NIH-PA Author Manuscript

Compd	pK_i (expt)	P-K_j (pred)	residual
59	7.60206	7.09237	0.50969
60	6.835647	6.86835	−0.0327
61	6.79588	6.69406	0.10182

[a]Molecules from the test set.